Exhibit A

Alignment: SEQ ID NO. 5 vs phosphohistidine domain of GWD from *Solanum tuberosum* (St-GWD), *Citrus reticulata* (CR-GWD) and *Arabidopsis thaliana* (AT-GWD)

Alignment **histid_Dom_GMD_PWD.msf** am 20.3.2009 →Output v.
histid_Dom_GMD_PWD kann markiert werden und mit Copy-Paste in Word **2000** (Nicks Compi) hineingefügt werden.

ClustalW 1.8 Parameters →fast pairwise alignment followed by multiple alignment		MView Parameters (output)	
ktuple=1 topdiag=5 window=5 pairgap=3 gapopen=10 gapextend=0.05	maxdiv=40 matrix: Gonnet nopgap nohgap	ruler: on coloring: group threshold: 80 width: 50 consensus: off consensus coloring: any consensus threshold: 100	consensus ignore: singleton consensus gaps: on consensus ref: 1 colormap: patent colorfile: -colorfile patent.map cons. colormap: - con_colormap patent
gapdist=8 (gaps < 8 residues from another gap are penalized more) endgaps (means 'OFF': gapdist does not apply for gaps at ends of sequence)			

```
Identities computed with respect to: (1) St-GWD
Colored by: consensus/80% and group property
Consensus Symbols                { Members in Class }

alcohol             =>  o        { S, T }
aliphatic           =>  l        { I, L, V }
aromatic            =>  a        { F, H, W, Y }
charged             =>  c        { D, E, H, K, R }
hydrophobic         =>  h        { A, C, F, G, H, I, K, L, M, R, T, V, W, Y }
negative            =>  -        { D, E }
polar               =>  p        { C, D, E, H, K, N, Q, R, S, T }
positive            =>  +        { H, K, R }
small               =>  s        { A, C, D, G, N, P, S, T, V }
tiny                =>  u        { A, G, S }
turnlike            =>  t        { A, C, D, E, G, H, K, N, Q, R, S, T }

                      1 [          . ] 12
St-GWD     100.0%       PDVLSHVSVRAR
CR-GWD     100.0%       PDVLSHVSVRAR
At-GWD     100.0%       PDVLSHVSVRAR
SEQISNO5    58.3%       LPHLSHLGVRAR
```


Download generierte MSF Datei

Exhibit B

Identification of a Novel Enzyme Required for Starch Metabolism in Arabidopsis Leaves. The Phosphoglucan, Water Dikinase[1[w]]

Oliver Kötting, Kerstin Pusch, Axel Tiessen, Peter Geigenberger, Martin Steup, and Gerhard Ritte*

Plant Physiology, Institute of Biochemistry and Biology, University of Potsdam, 14476 Golm, Germany (O.K., K.P., M.S., G.R.); and Max Planck Institute of Molecular Plant Physiology, 14476 Golm, Germany (A.T., P.G.)

The phosphorylation of amylopectin by the glucan, water dikinase (GWD; EC 2.7.9.4) is an essential step within starch metabolism. This is indicated by the starch excess phenotype of GWD-deficient plants, such as the *sex1-3* mutant of Arabidopsis (*Arabidopsis thaliana*). To identify starch-related enzymes that rely on glucan-bound phosphate, we studied the binding of proteins extracted from Arabidopsis wild-type leaves to either phosphorylated or nonphosphorylated starch granules. Granules prepared from the *sex1-3* mutant were prephosphorylated in vitro using recombinant potato (*Solanum tuberosum*) GWD. As a control, the unmodified, phosphate free granules were used. An as-yet uncharacterized protein was identified that preferentially binds to the phosphorylated starch. The C-terminal part of this protein exhibits similarity to that of GWD. The novel protein phosphorylates starch granules, but only following prephosphorylation with GWD. The enzyme transfers the β-P of ATP to the phosphoglucan, whereas the γ-P is released as orthophosphate. Therefore, the novel protein is designated as phosphoglucan, water dikinase (PWD). Unlike GWD that phosphorylates preferentially the C6 position of the glucose units, PWD phosphorylates predominantly (or exclusively) the C3 position. Western-blot analysis of protoplast and chloroplast fractions from Arabidopsis leaves reveals a plastidic location of PWD. Binding of PWD to starch granules strongly increases during net starch breakdown. Transgenic Arabidopsis plants in which the expression of PWD was reduced by either RNAi or a T-DNA insertion exhibit a starch excess phenotype. Thus, in Arabidopsis leaves starch turnover requires a close collaboration of PWD and GWD.

Starch, as the predominant storage carbohydrate in plants, is a major constituent of human and animal diets, and it is also an important raw material for various industrial processes (Slattery et al., 2000). Amylopectin, the major constituent of starch, contains varying amounts of covalently bound phosphate, depending upon plant species and organ. Phosphate is monoesterified to the C6 position (approximately two-thirds) and to the C3 position (approximately one-third). In addition, approximately 1% of the esterified phosphate may be linked to the C2 position (Tabata and Hizukuri, 1971). The total phosphorylation level of starch is quite low. In cereal endosperm starch, the amounts of Glc-6-P and Glc-3-P residues are at or below the detection limit and even in potato (*Solanum tuberosum*) tuber starch that is regarded as highly phosphorylated only 0.2% to 0.5% of the Glc residues are phosphorylated (Tabata and Hizukuri, 1971; Blennow et al., 2002). In Arabidopsis (*Arabidopsis thaliana*) leaf starch approximately 1 in 1,000 Glc residues is phosphorylated (Yu et al., 2001). Phosphate monoesters in amylopectin strongly affect starch functionality, and high phosphate contents are desirable for many industrial applications (Slattery et al., 2000; Blennow et al., 2002).

Phosphorylation of starch like polyglucans is catalyzed by the glucan, water dikinase (GWD, formerly designated as R1; EC 2.7.9.4; Ritte et al., 2002):

$$\text{glucan} + \text{ATP} + \text{H}_2\text{O} \rightarrow \text{glucan-P}_\beta + \text{AMP} + \text{P}_{\gamma i}.$$

The catalytic mechanism includes autophosphorylation of the dikinase protein. The β-P of ATP is firstly transferred to a His residue of GWD and then to either the C6 or the C3 position of a glucosyl unit (Ritte et al., 2002; Mikkelsen et al., 2004).

In GWD-deficient plants, not only starch phosphorylation but also starch breakdown is strongly impaired. In GWD antisense potato plants (Lorberth et al., 1998) as well as in the GWD-deficient starch-excess 1 (*sex1*) mutants of Arabidopsis (Yu et al., 2001), leaf starch contents at the end of the day are 3 to 5 times higher than those of the respective wild-type plants. More recently, it was shown that transitory starch in Chlamydomonas and potato is mainly phosphorylated during degradation (Ritte et al., 2004). This provides direct evidence for a link between the phosphorylation of starch and its degradation, but the underlying mechanisms remained obscure. It has been postulated that the activity of certain proteins that are involved in starch degradation depends on the pres-

[1] This work was supported by the Deutsche Forschungsgemeinschaft (grant nos. SFB 429 TP–B2 to M.S. and TP–B7 to G.R. and P.G.).

* Corresponding author; e-mail ritte@rz.uni-potsdam.de; fax 49–331–977–2512.

[w] The online version of this article contains Web-only data.

Article, publication date, and citation information can be found at www.plantphysiol.org/cgi/doi/10.1104/pp.104.055954.

ence of phosphate esters within starch (Yu et al., 2001; Ritte et al., 2002). However, until now, such enzymatic activities have never been documented. These proteins are expected to display a higher affinity to phosphorylated starch than to nonphosphorylated starch. This assumption provides a possible strategy for their identification.

Here we describe the discovery of a novel protein, which preferentially binds to phosphorylated starch. Its enzymatic function was investigated in vitro using purified protein and in vivo using transgenic plants.

RESULTS

Identification of a Novel Protein That Preferentially Binds to Phosphorylated Starch Granules in Vitro

To identify proteins whose activity depends on starch-bound phosphate esters, we compared binding of proteins to phosphorylated or nonphosphorylated starch granules. Phosphate free starch granules were isolated from leaves of the GWD-deficient Arabidopsis *sex1-3* mutant (Yu et al., 2001). Aliquots of the starch preparations were then in vitro phosphorylated using purified recombinant GWD from potato. Under the conditions applied, the phosphorylation levels range between 200 and 400 pmol P/mg starch. All the phosphate groups are located at the granule surface, since the recombinant GWD has no access to the granule interior. Phosphorylated and nonphosphorylated granules were then incubated with protein extracts from Arabidopsis wild-type leaves. Proteins bound to the granules were desorbed by a SDS-containing buffer and subsequently analyzed using SDS-PAGE and matrix-assisted laser-desorption ionization mass spectrometry (Fig. 1). Three proteins did bind preferentially to the phosphorylated starch. These were GWD (SEX1; At1g10760), cytosolic phosphorylase (Pho2; At3g46970), and an as-yet uncharacterized protein, preliminarily designated as OK1 (At5g26570). In the following we focus on the latter. OK1 turned out to be one of the two putative proteins with homology to GWD, whose existence was predicted from the Arabidopsis sequence (Yu et al., 2001). Database analysis using PlantGDB Blast (Dong et al., 2004) revealed the presence of putative OK1 orthologs in 14 different plant species including potato, tomato, barley, and rice.

Using primers designed for the At5g26570 gene, the full-length OK1 cDNA sequence was cloned. In the sequence thereby derived, 15 additional nucleotides (1,555–1,569) were found that were not present in the already existing corresponding National Center for Biotechnology Information (NCBI) entry (NM_122538). The OK1 cDNA sequence was submitted to EMBL (accession no. AJ635427).

OK1 and GWD amino acid sequences were compared using the BLAST 2 Sequences tool (Tatusova and Madden, 1999). The C-terminal regions, ranging from amino acid 611 to 1,196 (OK1), and 860 to 1,398

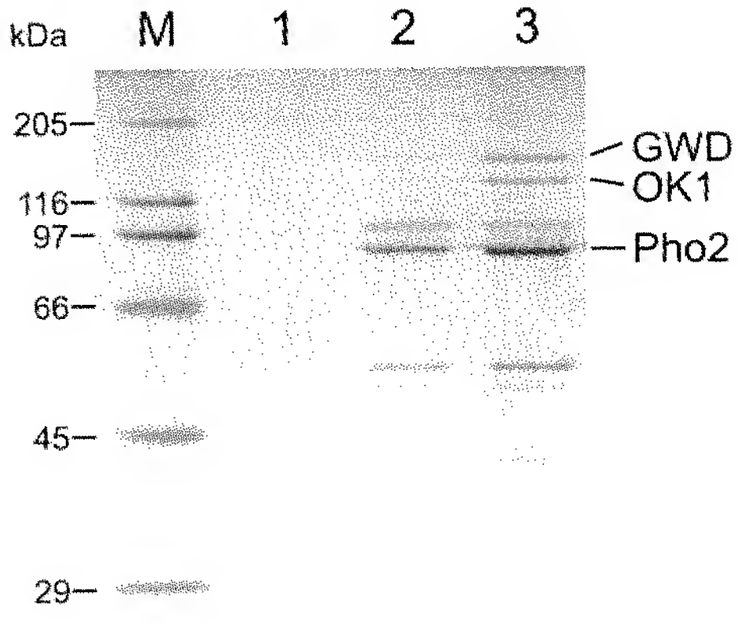

Figure 1. In vitro binding of proteins to phosphorylated or nonphosphorylated starch granules. Protein extracts from ecotype Columbia leaves were incubated with either nonphosphorylated (2) or previously in vitro phosphorylated (3) starch granules from *sex1-3* leaves. Granules were washed, and bound proteins were released with SDS sample buffer and separated by SDS-PAGE. 1, In vitro phosphorylated starch granules incubated without extract; M, molecular mass marker. Three proteins with higher affinity to phosphorylated starch are indicated (GWD, OK1, and Pho2).

(GWD), displayed 25% amino acid identity, and 41% sequence similarity. No similarity could be detected in the N-terminal regions. The overall amino acid identity, as analyzed with the AlignX program (Vector NTI, Invitrogen, Karlsruhe, Germany), is 14%, and sequence similarity is 24%.

Analysis of the OK1 sequence using TargetP (Emanuelsson et al., 2000) reveals a high probability for the existence of a signal peptide directing the protein to plastids (score 0.992). Three further domains could be detected (Fig. 2A). A starch binding domain (CBM 20) is located at the N-terminal region of OK1. The C terminus of OK1 displays homology to the nucleotide binding domains of the dikinases pyruvate, phosphate dikinase (PPDK; EC 2.7.9.1), phospho*enol*-pyruvate (PEP)-synthase (pyruvate, water dikinase; EC 2.7.9.2), and GWD (Marchler-Bauer et al., 2003). A region with significant homology to the phosphohistidine domains of these dikinases is also present in the OK1 sequence (Fig. 2B).

OK1 Is Localized in Plastids

The prediction of OK1 being a plastidic protein by the bioinformatic programs was further strengthened by western-blot analysis of extracts made from Arabidopsis leaf protoplasts and chloroplasts isolated from protoplasts. Equal amounts of protein were analyzed by SDS-PAGE and western blot using specific antibodies raised against ADP-Glc-pyrophosphorylase (AGPase, plastidic marker), PEP-carboxylase (cytosolic marker), and OK1. As shown in Figure 3 for both AGPase and OK1, an immunosignal was obtained in the chloroplast fraction, whereas there was hardly any signal in the protoplast fraction. In contrast,

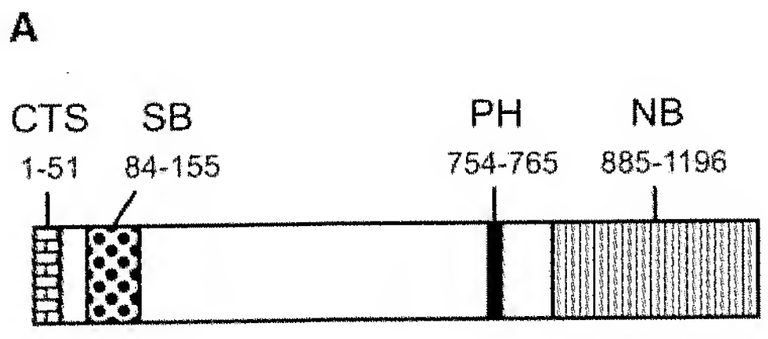

Figure 2. OK1 contains a starch binding domain and domains typical for dikinases. A, Protein domains of the OK1 protein. The amino acid number indicates the location of the respective domain within the protein. CTS, Chloroplast targeting signal; SB, starch binding domain CBM 20; PH, putative phosphohistidine domain; NB, nucleotide binding domain. B, Alignment of the putative phosphohistidine domains of OK1 and different dikinases. The putative phosphohistidine regions of GWDs from Arabidopsis (*At*), potato (*St*), and *Citrus reticulata* (*Cr*) were aligned with the putative phosphohistidine regions of PPDKs from *Zea mays* (*Zm*) and *E. coli*, pyruvate, water dikinase (PPS) from *E. coli*, and the homologous region of OK1. Identical amino acids in black, conserved in gray boxes. The putative phosphohistidine is printed in boldface.

the cytosolic marker PEP-carboxylase was exclusively detected in the protoplast fraction. Nonaqueous fractionation of Arabidopsis leaf material and subsequent western-blot analysis also indicates that OK1 resides in plastids (data not shown). Furthermore, OK1 is found in the Arabidopsis chloroplast protein database (http://www.pb.ipw.biol.ethz.ch/index.php?toc=91; Kleffmann et al., 2004), thereby providing another line of evidence for plastidic localization of this protein. Thus, the interaction of OK1 with phosphorylated starch may well be of physiological relevance.

OK1 Is a Phosphoglucan, Water Dikinase

A vector was constructed allowing the expression of OK1 containing a 6×His tag at the N terminus in *Escherichia coli* and one step purification of the recombinant protein using a Ni-NTA agarose resin. The full-size OK1 protein is clearly predominant in the resulting protein fraction (Supplemental Fig. 1). Because of the similarity between OK1 and GWD, we tested whether or not OK1 also displays starch phosphorylating activity. As for the in vitro binding assay, nonphosphorylated or phosphorylated starch granules served as substrates. OK1 was indeed able to transfer ^{33}P from [$\beta\gamma$-^{33}P]ATP to starch. Most remarkably, however, the activity strictly depended on a preceding phosphorylation of the granules by recombinant potato GWD (Fig. 4A). We never observed OK1-catalyzed phosphorylation of the unmodified phosphate free *sex1-3* starch ($n = 7$). Similar to GWD, OK1 transfers the β-P of ATP to starch. There was no significant phosphate incorporation of labeled phosphate into the starch substrate if [γ-^{33}P]ATP served as phosphate donor (Fig. 4B).

To study the fate of the γ-P of ATP, we analyzed OK1-catalyzed incorporation of β-P into phosphorylated starch using [β-^{33}P]ATP as phosphate donor as well as a possible release of γ-P-ortophosphate into the soluble phase using [γ-^{33}P]ATP. For comparison, the same experiment was also conducted using recombinant potato GWD, for which we have shown before that water is the acceptor of the γ-P (Ritte et al., 2002). As shown in Table I, in both cases comparable amounts of phosphate were incorporated into starch or released as inorganic phosphate into the soluble phase, respectively. In both samples, the amount of γ-P released exceeded that of β-P detected in the starch fraction by about 20% to 30%. However, it is possible that the amount of incorporated phosphate is underestimated due to some loss of starch granules during the extensive washing procedure.

We conclude that OK1 is a phosphoglucan, water dikinase (PWD) that transfers the β-P of ATP to a phosphoglucan and the γ-P of ATP to water:

$$\text{Glucan-P}_n + \text{ATP} + \text{H}_2\text{O} \rightarrow \text{Glucan-P}_{n+1} + \text{AMP} + \text{P}_i.$$

Therefore, we replace the preliminary term OK1 with PWD.

Under standard assay conditions (10 mg phosphorylated starch granules/mL, 25 μM ATP, 30 min), a linear correlation between PWD protein amount and phosphate incorporation into the substrate is only observed at low protein concentrations (<0.1 μg/mg starch; Supplemental Fig. 2A). For 0.05 μg PWD/mg starch, we calculated an activity of 2.55 nmol min^{-1}

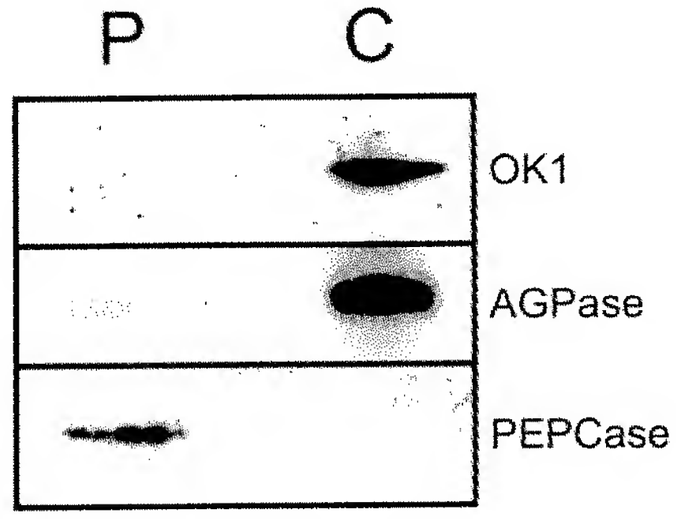

Figure 3. OK1 is located in chloroplasts. Equal amounts of protein extracted from Arabidopsis leaf protoplasts (P) and chloroplasts (C), respectively, were separated by SDS-PAGE and examined by immunoblot analysis using antibodies against OK1, AGPase (plastidic marker), and PEPCase (cytosolic marker).

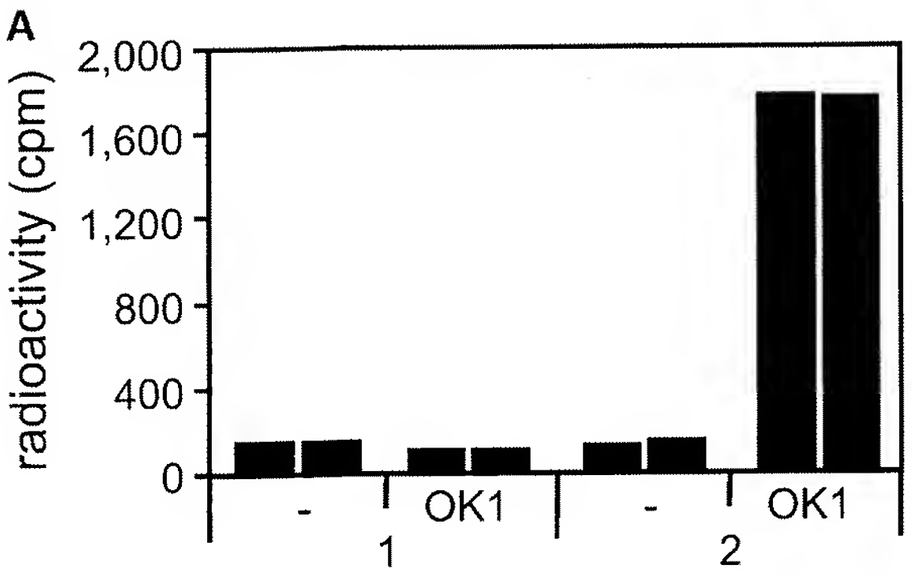

Figure 4. In vitro activity assay with recombinant OK1 protein. A, OK1 phosphorylates phosphoglucans but not phosphate free glucans. One microgram recombinant OK1 protein was incubated for 15 min with 25 μM ATP containing 0.5 μCi [$\beta\gamma$-^{33}P]ATP and 5 mg of either non-phosphorylated (1) or in vitro phosphorylated (2) starch granules from *sex1-3* leaves. The radioactivity incorporated into the granules was counted. -, Control without protein. Bars represent the individual measurements of two parallel samples. B, OK1 transfers the β-P of ATP to phosphoglucans. Recombinant OK1 protein (2.2 μg) was incubated for 1 h with 4.2 mg in vitro phosphorylated starch granules and either [$\beta\gamma$-^{33}P]ATP or solely [γ-^{33}P]ATP (0.5 μCi in both cases). ATP concentration, 25 μM. The radioactivity incorporated into the granules was counted. -, Control without protein.

(mg protein)$^{-1}$. This value is slightly underestimated because [$\beta\gamma$-^{33}P]ATP was used that contains ≥80% of label in the β-position (Ritte et al., 2003). The PWD activity is similar to the specific activity of potato GWD with soluble potato amylopectin (Ritte et al., 2002) and also to the activity of GWD with unmodified *sex1-3* starch granules as substrate (data not shown).

For a more quantitative analysis, starch granules containing different amounts of phosphate esters (9, 49, and 215 pmol P/mg starch) were reacted with PWD (Supplemental Fig. 2B). The granule preparation with the highest phosphate content was the most efficient phosphate acceptor. However, PWD activities with the different substrates varied about 6-fold, whereas the level of prephosphorylation varied about 24-fold. Thus, there is no linear relation between the phosphate content of a polyglucan and its capacity to serve as phosphate acceptor for PWD.

As observed with nonphosphorylated *sex1-3* starch granules PWD was unable to phosphorylate solubilized *sex1-3* starch (Supplemental Fig. 2C). However, even solubilized *sex1-3* starch that had been prephosphorylated by GWD proved to be an extremely poor substrate for PWD (Supplemental Fig. 2C). The same holds true for soluble potato starch (Sigma S-2004) although it contains approximately 15 nmol P/mg starch (data not shown). Possibly, the structure of the starch granule or of the surface of the particle is also important for the PWD activity.

PWD Is Capable of Autophosphorylation

A phosphohistidine is an intermediate in the dikinase type reactions catalyzed by PPDK (Goss et al., 1980), PEP-synthase (Narindrasorasak and Bridger, 1977), and GWD (Ritte et al., 2002; Mikkelsen et al., 2004). The β-P of ATP is firstly transferred to the His residue and then to pyruvate (in case of PPDK and PEP-synthase) or a glucan (in case of GWD). As mentioned above an amino acid stretch displaying homology to the phosphohistidine domains of these enzymes is also present in PWD. To study whether PWD follows a similar mechanism, we incubated the purified protein with either [$\beta\gamma$-^{33}P]ATP or [γ-^{33}P]ATP in the absence of a phosphoglucan and analyzed a possible autophosphorylation by SDS-PAGE and autoradiography. Labeling of the PWD protein was observed only in the samples containing [$\beta\gamma$-^{33}P]ATP but not in those containing [γ-^{33}P]ATP (Fig. 5). Thus, PWD phosphorylates itself with the β-P. The phosphorylation was heat labile, acid labile but rather stable in alkali (Fig. 5). This is consistent with a phosphohistidine being formed, since phosphoserine, phosphotyrosine, and phosphothreonine are heat stable, acid stable, but alkali labile (Rosenberg, 1996). The results strongly indicate that the β-P of ATP is firstly transferred to a His residue of PWD and afterward to the phosphoglucan.

PWD Phosphorylates Preferably the C3 Position of the Glucosyl Residues in Phosphoglucans

To analyze which positions of the Glc residues are phosphorylated by PWD, starch was prephosphory-

Table I. *OK1 transfers the γ-P of ATP to water*

Recombinant OK1 or GWD protein (2.2 μg each) were incubated with in vitro phosphorylated *sex1-3* starch granules for 80 min. Either [β-^{33}P]ATP or [γ-^{33}P]ATP of identical specific radioactivity served as phosphate donor. The incorporation of β-P into starch (control, buffer instead of protein) and the release of γ-P_i into the soluble phase (control, no starch) was determined.

	[β-^{33}P]-Incorporation	[γ-^{33}P]-Release
	pmol	*pmol*
OK1	34.3	42.8
GWD	123.3	172.0

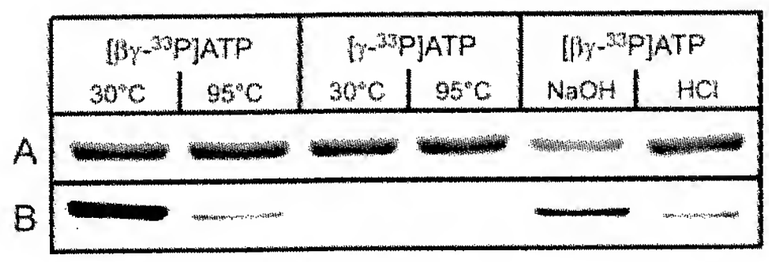

Figure 5. Autocatalytic phosphorylation of recombinant PWD (OK1). Recombinant PWD protein was incubated in the absence of starch granules with either [$\beta\gamma$-^{33}P]ATP or solely [γ-^{33}P]ATP (1.4 μCi/μg protein each). Heat stability of the phosphorylated PWD was tested by incubation of the samples at either 30°C for 30 min or 95°C for 5 min. Acid or base stability of the phosphorylated PWD protein was assayed by incubation in 0.5 N NaOH or 0.5 N HCl for 30 min at RT, followed by denaturation in SDS sample buffer for 30 min at 30°C. Samples were separated by SDS-PAGE (1.8 μg PWD protein/lane) and visualized by either Coomassie Blue staining (A) or autoradiography (B).

lated by GWD (using unlabeled ATP) and then phosphorylated by PWD using ^{33}P-ATP. For comparison, an experiment in which starch was solely phosphorylated by GWD (using labeled ATP) was also performed. Following in vitro phosphorylation, Glc and Glc-Ps were released from starch by means of acid hydrolysis. To separate Glc-6-P and Glc-3-P, the samples were subjected to high performance anion-exchange chromatography with pulsed amperometric detection (HPAEC-PAD). Since the extent of in vitro phosphorylation is too low to allow for reliable amperometric detection of the Glc-Ps thereby formed we added authentic Glc-6-P and Glc-3-P as standards. Fractions were collected and the radioactivity was counted.

In contrast to GWD, which phosphorylates preferably the C6-position, PWD phosphorylates predominantly the C3-position (Fig. 6). Approximately 70% of the radioactivity incorporated into starch by PWD coeluted with Glc-3-P in two independent experiments. It has to be considered that Glc-3-P is a rather acid labile compound. The investigation of starch bound phosphate esters by acid hydrolysis of granular starch and subsequent analysis of the products by HPAEC-PAD was adapted from Blennow et al. (1998). They estimated that during 2 h of acid hydrolysis approximately 20% of the Glc-3-P is dephosphorylated. We found that 24% of the radioactivity in the starch hydrolysate was present as inorganic phosphate using the modified Parvin and Smith method (see "Materials and Methods"). In contrast, if starch was hydrolyzed following in vitro phosphorylation with GWD less than 5% of the label were present as inorganic phosphate. When ^{32}P-orthophosphate was subjected to HPAEC-PAD approximately 20% of radioactivity coeluted with Glc-6-P the remaining 80% eluted in the fraction between Glc-6-P and Glc-3-P (data not shown). Thus, in the hydrolyzed PWD product the radioactivity eluting ahead of the Glc-3-P peak (Fig. 6) can, at least in part, be attributed to orthophosphate that is released from Glc-3-P during sample processing.

In Vitro Analysis of PWD Purified from Leaves Confirms the Results with the Heterologously Expressed Protein

Analysis of the recombinant PWD has revealed unique features of this enzyme. However, it has to be kept in mind that the recombinant PWD protein is not identical to PWD in plants. Since the length of the transit peptide is only predicted but not exactly known the complete coding sequence of PWD was used to generate the expression vector. Furthermore, the protein contains an N-terminal His tag and a single amino acid replacement (see "Materials and Methods"). Therefore, we analyzed the plant-derived protein in addition to the recombinant PWD. The protein was partially purified by ammoniumsulfate precipitation and affinity chromatography using immobilized maltoheptaose (Supplemental Fig. 3A). As has been shown for the recombinant protein, activity of PWD purified from leaves strictly depended on a preceding phosphorylation by GWD (Supplemental Fig. 3B) and phosphorylation predominantly (or exclusively) occurs at the C3-position of the Glc residues (Supplemental Fig. 3C).

Reduction of PWD in Transgenic Plants Causes a Starch Excess Phenotype

To investigate the in vivo function of PWD, an RNA interference (RNAi) construct was designed to repress the activity of this protein in Arabidopsis. Fifteen transgenic lines were analyzed by western blot, all of which proved to be strongly reduced in PWD protein (data not shown). Five of these lines were examined in more detail. As shown in Figure 7A the PWD protein amount in the RNAi lines 1 to 4 is below the limit of

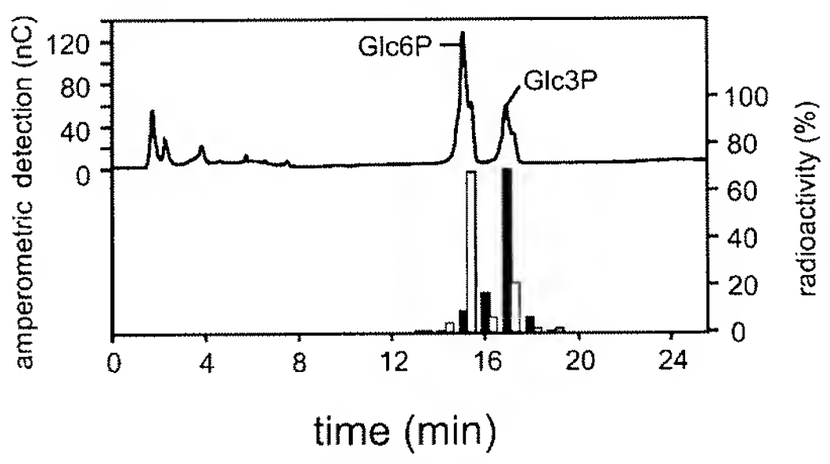

Figure 6. PWD (OK1) phosphorylates preferentially the C-3 position of the Glc units. Recombinant PWD and GWD protein (first experiment: 25 μg PWD, 5 μg GWD; second experiment: 4.2 μg PWD, 0.7 μg GWD), respectively, were incubated with in vitro phosphorylated *sex1-3* starch granules and [$\beta\gamma$-^{33}P]ATP for 1 h. Starch granules were hydrolyzed. Aliquots of the hydrolyzates were supplemented with Glc-3-P and Glc-6-P as internal standards and subjected to HPAEC-PAD analysis (top section). Fractions were collected every minute (1 mL), except for Glc-3-P and Glc-6-P fractions, which were collected quantitatively in separate fractions. Radioactivity in the collected fractions was counted. The relative distribution of radiolabel was calculated as percentage of total radioactivity in all collected fractions (bottom section). GWD, White bars; PWD, black bars. Values are means of two independent experiments.

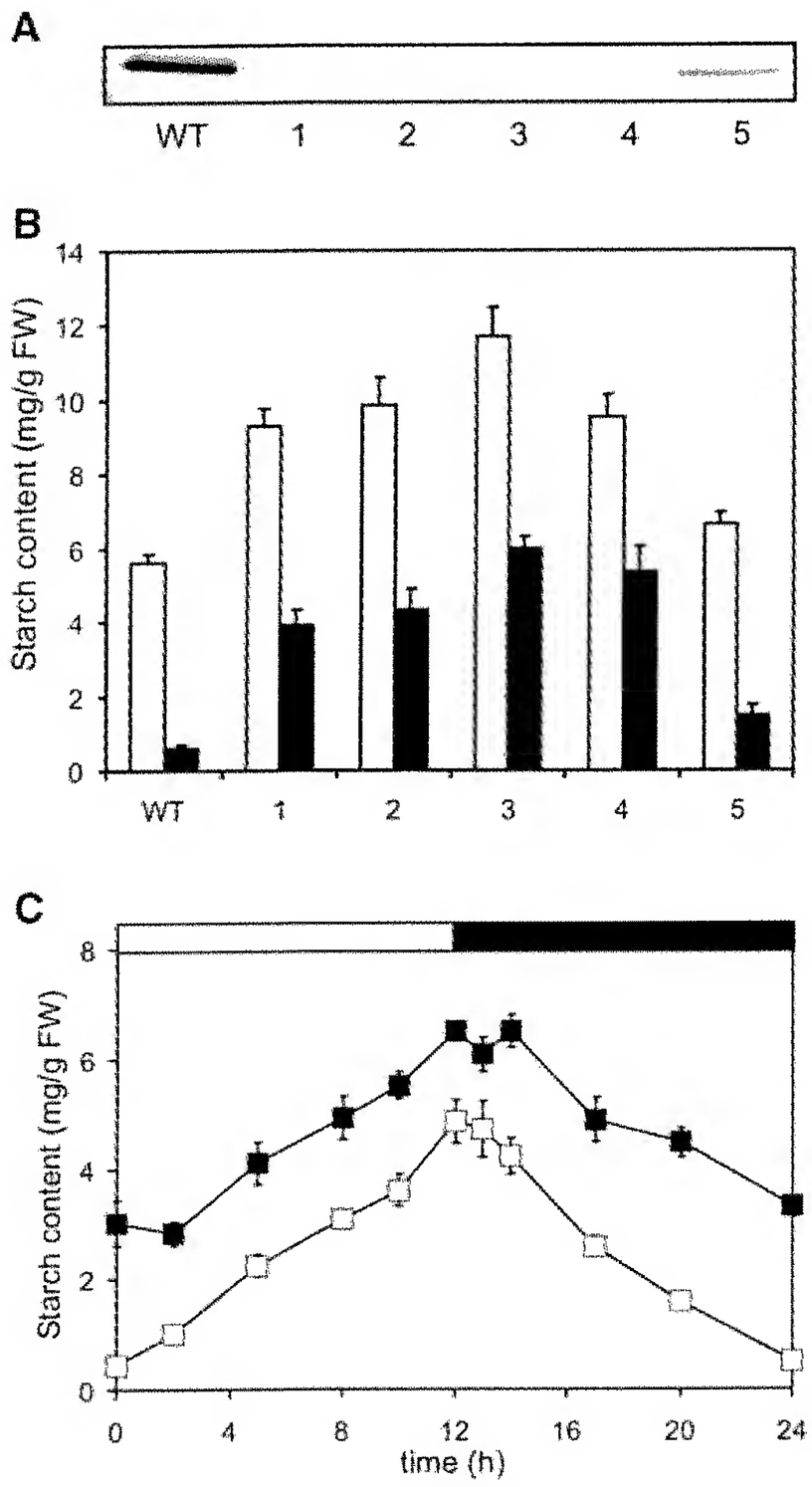

Figure 7. Transgenic plants with reduced PWD (OK1) protein exhibit a starch excess phenotype. A, The PWD protein level is decreased in PWD RNAi plants. Leaf samples of five PWD RNAi lines and wild type were harvested at the end of the light period. Proteins were extracted and 40 μg each were separated by SDS-PAGE and examined by immunoblot analysis using an anti-PWD antibody. WT, Wild type; 1 to 5, PWD RNAi lines 1 to 5. B, Starch content in leaves of wild-type and PWD RNAi lines. Plants were grown in a 12-h-light/12-h-dark cycle. Samples were taken at the end of the light (white bars) and dark period (black bars), respectively. Values are means ± SE; $n = 4$ plants. 1 to 5, PWD RNAi lines; WT, wild type; FW, fresh weight. C, Starch content in leaves of wild type and PWD knockout mutant. All leaves of wild-type plants (white symbols) or *pwd* plants (black symbols) were harvested at the times indicated. Values are means ± SE; $n = 4$ plants.

detection using western-blot analysis. In line 5 PWD expression is reduced by at least 75%. The analysis of starch contents in these plants revealed a metabolic phenotype for PWD. At the end of the day, the PWD-deficient plants contained up to 2 times more starch than ecotype Columbia wild type (Fig. 7B). Starch is nearly completely remobilized during night in wild-type but not in the transgenic plants. In the less inhibited RNAi-line 5, starch amounts are only slightly increased compared with wild-type plants. Thus, the extent of PWD inhibition correlates with the effect on starch content.

We also obtained an insertion mutant (SALK_110814) and selected a homozygous line for the At5g26570 gene. No PWD protein could be detected in the mutant (data not shown). As observed with the RNAi plants, the PWD knockout mutant (*pwd*) contains considerably more starch than wild-type plants throughout the day/night cycle (Fig. 7C). Starch turnover occurred in the PWD-deficient plants, but the rate of starch degradation in the *pwd* plants was lower than that of the wild-type plants (Fig. 7C). This effect was also observed using an independent batch of plants grown under a 14-h-light period (data not shown).

The high starch phenotype resembles that of the GWD-deficient *sex1* mutants. However, when grown under the same conditions the *sex1* mutants accumulate more starch than the *pwd* plants. The lack of PWD had a minor effect on plant development, whereas the GWD knockout mutant *sex1-3* is strongly retarded in growth when cultivated under a 12-h-light/12-h-dark regime (Supplemental Fig. 4).

Starch-bound phosphates in wild-type and PWD RNAi plants (lines 1–5) were analyzed by HPAEC-PAD and quantification of the peak areas following acid hydrolysis of the starch granules. The Glc-6-P:Glc-3-P ratio increased from 2.1 in wild type to 2.5 in the transgenic plants (mean of lines 1–5), ranging from 2.2 in line 5 to 2.7 in line 1. This increase, however, was caused by slightly elevated Glc-6-P levels, whereas the Glc-3-P content was essentially unchanged (data not shown). The Glc-6-P:Glc-3-P ratio in starch of *pwd* plants was also increased compared with wild type (data not shown). It has to be considered that the Glc phosphate levels in starch hydrolyzates mainly reflect starch phosphorylation during biosynthesis and not the transient phosphorylation of the granule surface during breakdown (Ritte et al., 2004).

PWD Binds to Leaf Starch Granules during Their Breakdown

To analyze whether binding of PWD to transitory starch is affected by the physiological state of the cell, granule-bound and soluble protein was extracted from leaves of wild-type plants that had been harvested either in the light or dark period. As revealed by western-blot analysis, binding of PWD to the surface of transitory starch granules strongly increases during starch mobilization in darkness (Fig. 8). In contrast, the PWD level in the buffer soluble fraction was equal in the light and dark samples. Binding of GWD to transitory starch in Arabidopsis also significantly increases in darkness (Fig. 8), in agreement with earlier results using leaves of potato and pea, respectively (Ritte et al., 2000a).

DISCUSSION

The factors and mechanisms leading to the degradation of the crystalline starch granule are largely

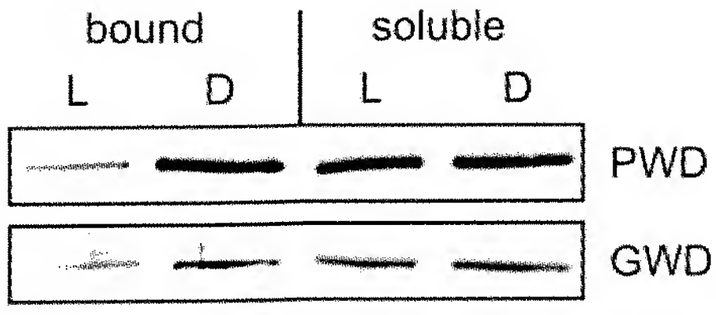

Figure 8. PWD (OK1) binds to the surface of leaf starch granules during their degradation. Leaves of Arabidopsis wild-type plants were harvested 2 h before (L) and 2 h after the end of the light period (D). Soluble proteins and starch were extracted. Proteins bound to the surface of the starch granules were released by incubation in SDS-sample buffer at RT. Proteins released from 6.5 mg starch (bound) or 40 μg of soluble protein (soluble) were subjected to SDS-PAGE and immunoblot analysis using antibodies against PWD and GWD. The experiment was repeated with an independently grown batch of plants and yielded the same result.

unknown, but there is increasing evidence that phosphorylation of starch by GWD is involved (Zeeman et al., 2004). In a first approach to unravel the link between the GWD-catalyzed phosphorylation of starch and the degradation of the polyglucans, we searched for proteins displaying enhanced affinity to phosphorylated starch compared with nonphosphorylated starch. We identified a novel protein (PWD) that preferentially binds to phosphorylated starch and is capable of glucan phosphorylation. The reaction catalyzed by PWD differs from that of GWD and, thus, represents a novel enzymatic activity. In contrast to GWD, phosphorylating activity of PWD was only observed using substrates that already contained glucan-bound phosphate. In vitro phosphorylated *sex1-3* granules were a suitable substrate for PWD, whereas we did not detect PWD-catalyzed phosphate incorporation into the unmodified phosphate free *sex1-3* starch. Likewise, starch granules from wheat (Sigma S-5127) were not phosphorylated by PWD, but following prephosphorylation with GWD they can serve as substrate for PWD (data not shown).

Why is PWD active only on phosphorylated starch? It is reasonable to assume that PWD either phosphorylates glucan chains that were previously phosphorylated by GWD, or it phosphorylates unphosphorylated chains within a phosphorylated matrix. Analysis of the phosphorylated glucan chains following in vitro phosphorylation with ^{33}P-ATP shows that the latter predominates. Approximately 80% of the incorporated label was recovered in singly phosphorylated glucan chains; the remaining radioactivity was found in doubly phosphorylated chains. Probably phosphate incorporation by GWD locally alters the starch structure and thereby generates phosphorylation sites that can be used by PWD.

Whereas activity of PWD strictly depends on the presence of glucan bound phosphate binding of the protein to carbohydrates does not. PWD can bind to the unmodified *sex1-3* granules, albeit with low efficiency. The protein also binds to immobilized maltoheptaose (S. Orzechowski, unpublished data), and we made use of this to enrich the protein from leaf extracts. These maltoheptaose beads were also not at all phosphorylated by the recombinant PWD (data not shown).

An important difference between PWD and GWD is the site of phosphate incorporation. GWD phosphorylates both the C3 and the C6 position, with a clear preference of the latter. In contrast, PWD phosphorylates preferably the C3 position (Fig. 6). A low extent of C6-phosphorylation cannot be ruled out; the same holds true for C2-phosphorylation. It has been suggested by Tabata and Hizukuri (1971) that about 1% of the phosphate in potato tuber starch could be linked to the C2 position. Glc-2-P is far more acid labile than Glc-3-P (Tabata and Hizukuri, 1971; Kokesh et al., 1978), and complete dephosphorylation during acid hydrolysis as applied here can be expected. Therefore, we cannot exclude that Glc-2-P residues may also be formed by PWD (or GWD as well). NMR analysis could provide further information whether or not C3 is the single phosphorylation site of PWD. However, due to the low level of PWD-catalyzed phosphate incorporation in vitro and the high background level of phosphate esters in the starch substrate, NMR-analysis of the PWD products is not practicable at present.

Starch is phosphorylated during its biosynthesis (Nielsen et al., 1994; Wischmann et al., 1999) but in addition also during its degradation (Ritte et al., 2004). The amounts of Glc-6-P and Glc-3-P determined in hydrolyzed starch mainly reflect starch phosphorylation during starch synthesis (Ritte et al., 2004). The absolute level of starch-bound Glc-3-P is not significantly altered in the PWD-deficient plants. This may indicate that the enzyme is not involved in biosynthesis associated phosphorylation. However, GWD can attach phosphate at both C3 and C6 positions of Glc residues in amylopectin, and may thus partly compensate for lacking PWD activity. The amount of GWD protein is unaltered in the PWD-deficient plants as revealed by western-blot analysis (data not shown), but it is possible that more glucan targets become available for GWD if PWD is lacking.

The increased phosphorylation of the granule surface during breakdown of starch in chloroplasts (Ritte et al., 2004) should favor activity of PWD during starch mobilization. In fact, binding of PWD to transitory starch granules is strongly increased during degradation of the starch particle (Fig. 8). Phosphorylation during starch mobilization is restricted to the outermost layer of the granule, and the phosphate esters introduced during breakdown underlie a rapid turnover (Ritte et al., 2004). Consequently, the reduction of C3-phosphorylation during the period of starch mobilization is not expected to noticeably affect the total Glc-3-P level of starch.

The starch excess phenotype observed in the PWD-deficient plants demonstrates that this enzyme plays an important metabolic role, and lack of PWD-catalyzed starch phosphorylation cannot be (fully) compensated for by other enzymes. Since the activity

of PWD depends on a preceding starch phosphorylation by GWD, the lack of GWD in mutant plants should also abolish starch phosphorylation by PWD. Consistently, no Glc-3-P residues could be detected in starch of the GWD-free Arabidopsis mutant *sex1-3* (Yu et al., 2001). The starch excess phenotype in the GWD-deficient plants is probably attributable to a combined reduction of GWD and PWD activity, which might explain the more severe phenotype compared with PWD mutants.

Further studies are required to explore the link between phosphorylation and degradation of starch. It has recently been reported that the in vitro degradation of granules isolated from turions of the duckweed by starch associated proteins (including a putative GWD ortholog) could be increased by addition of ATP, thereby enabling starch phosphorylation (Reimann et al., 2004). We have obtained similar results using potato leaf starch. Furthermore, we know from in vitro studies that as-yet unidentified proteins exist in Arabidopsis that degrade starch more efficiently if it is phosphorylated (G. Ritte, unpublished data). Future work will focus on the characterization of these proteins to evaluate their role in starch degradation in vivo.

We propose that the newly identified PWD acts downstream of GWD and is involved in starch breakdown in leaves. Based on molecular modeling it has been suggested that phosphate linked to the C6 position aligns with the surface of double helical motifs in amylopectin, whereas phosphate esterified to the C3-position protrudes from the double helical structure. Thus, double helix packing should be more affected by C3-phosphorylation (Blennow et al., 2002; Engelsen et al., 2003). In addition to the GWD-catalyzed phosphate incorporation, phosphorylation of the C3 position by PWD could play an important role in rendering the starch granule accessible for degrading enzymes by disturbing the helix packing and increasing the hydrophilicity.

MATERIALS AND METHODS

Plant Material and Growth Conditions

Arabidopsis (*Arabidopsis thaliana*) plants were cultivated in a growth cabinet under controlled conditions (12 h light/12 h dark, 20°C/16°C, 60%/70% relative humidity [day/night], and approximately 150 μmol quanta m^{-2} s^{-1}). Seeds of the mutant SALK_110814 were obtained from the Nottingham Arabidopsis Stock Center (http://arabidopsis.info, Nottingham, UK). Seeds of the Arabidopsis *sex1-1* and *sex1-3* mutants (Yu et al., 2001) were a kind gift of Dr. Samuel Zeeman (University of Berne, Switzerland).

Chemicals and Enzymes

[γ-^{33}P]ATP (10 mCi/mL; 3,000 Ci/mmol), [β-^{33}P]ATP (10 mCi/mL; 800 Ci/mmol), and [^{32}P]phosphoric acid (54 mCi/mL, carrier free) were all purchased from Hartmann Analytic (Braunschweig, Germany). Glc-3-P was synthesized as described elsewhere (Ritte et al., 2002).

Preparation of Leaf Starch Granules

Leaves (10–30 g) were frozen in liquid nitrogen and homogenized in a mortar. For the analysis of granule-bound proteins in vivo, starch was extracted as described (Ritte et al., 2000a). For structural analysis of starch and for isolation of starch granules serving as raw material for binding or activity assays, the above method was modified as follows. The extraction buffer consisted of 20 mM HEPES-KOH, pH 8.0, 0.2 mM EDTA, 0.5% (w/v) Triton X-100. Following passage through a Percoll cushion (Ritte et al., 2000a), the starch pellet was washed once in extraction buffer. Proteins bound to the starch granule surface were then removed by incubation with 0.5% (w/v) SDS on a rotating wheel (approximately 10 μL SDS-solution/mg starch, 3 × 15 min, room temperature [RT]). Subsequently SDS was removed by washing the granules three times (15 min each) in 50 mM HEPES-KOH, pH 7.2, and once in water. Starch granules were either used immediately or dried under vacuum and stored at −20°C.

Radioactive Starch Phosphorylation Assay

Five milligrams starch were resuspended in 50 mM HEPES-KOH, pH 7.5, 1 mM EDTA, 6 mM $MgCl_2$, 0.025% Triton X-100, and radiolabeled ATP as indicated in a total volume of 0.5 mL if not otherwise stated. The radiolabel was either [β-^{33}P]ATP, [γ-^{33}P]ATP, or [$\beta\gamma$-^{33}P]ATP. The latter was obtained by enzymatic randomization of [γ-^{33}P]ATP according to Ritte et al. (2004) and is predominantly labeled at the β-position (Ritte et al., 2003). Reactions were started by addition of protein. The samples were agitated on a rotating wheel at RT for the times indicated, and the reaction was terminated by adding SDS (final concentration, 2%). The starch was washed two times in water and at least four times in 2 mM ATP as described (Ritte et al., 2004). Subsequently, the granules were resuspended in 0.1 mL water, mixed with 3 mL scintillation fluid, and the radioactivity was counted.

In Vitro Phosphorylation of Leaf Starch Granules by Recombinant GWD

Unless otherwise stated, dried Arabidopsis *sex1-3* leaf starch granules were resuspended in 50 mM HEPES-KOH, pH 7.5, 1 mM EDTA, 6 mM $MgCl_2$, 0.5 mM ATP, and purified recombinant potato (*Solanum tuberosum*) GWD (Ritte et al., 2002) was added to give final concentrations of 10 mg starch/mL buffer and 0.25 μg GWD/mg starch. Following incubation overnight on a rotating wheel, the reaction was stopped by adding SDS (final concentration, 2%). Removal of recombinant protein and washing of starch was done as described above (starch granule preparation). The amount of phosphate incorporated was estimated in parallel samples in which, however, [$\beta\gamma$-^{33}P]ATP (0.5–1 μCi) was included under otherwise identical conditions. In the [$\beta\gamma$-^{33}P]ATP preparation, ≥80% of the label is normally present in the β-position (Ritte et al., 2003). Estimations were done as if 100% of the label were present in the β-position. Thus, the indicated phosphate incorporation is slightly underestimated.

Protein Extraction

Arabidopsis leaves were harvested and immediately frozen in liquid nitrogen. Leaves were ground in a mortar, and 3 to 4 volumes (v/w) binding buffer (50 mM HEPES-KOH, pH 7.2, 1 mM EDTA, 2 mM dithioerythritol, 2 mM benzamidine, 2 mM ε-aminocaproic acid, 0.5 mM phenylmethylsulfonylfluoride, 0.02% Triton X-100) were added (4°C). All following steps were carried out at 4°C. Plant material was additionally homogenized in an Ultraturrax (2 × 10 s, maximum speed), passed through a 100-μm nylon mesh, and centrifuged for 20 min (20,000*g*). Proteins were precipitated by adding ammonium sulfate (75% saturation). Following centrifugation, the precipitate was resolved in binding buffer and desalted using Sephadex G25 (Amersham Bioscience, Freiburg, Germany).

In Vitro Binding Assay

Both in vitro-phosphorylated and nonphosphorylated *sex1-3* leaf starch granules (50 mg each) were hydrated in binding buffer and were then mixed with freshly prepared Arabidopsis protein extract (total volume 0.8 mL, 4–10 mg protein mL^{-1}). Following incubation for 15 min at 4°C, unbound proteins were removed by centrifugation through a 4-mL Percoll-cushion (see above). The pelleted starch was washed in binding buffer (2 × 5 min, 4°C). Bound proteins were solubilized by incubating the starch granules with SDS sample buffer (62.5 mM Tris-HCl, pH 6.8, 2% [w/v] SDS, 10% [w/v] glycerol, 0.01% [w/v] bromphenol blue) for 15 min at RT with shaking. After centrifu-

gation (5 min, 20,000*g*), the supernatant was transferred to a new tube and incubated at 95°C for 5 min. Equal amounts of both samples were separated by SDS-PAGE (9% acrylamide in the separation gel). Gels were stained with colloidal Coomassie Blue (Roth, Karlsruhe, Germany), and protein bands were cut out and subjected to tryptic digestion and matrix-assisted laser-desorption ionization mass spectrometry analysis as described (Ritte et al., 2000b).

Antibodies

Antibodies were raised in rabbits. A polyclonal antibody against the purified recombinant OK1 (PWD) was produced by Eurogentec (Seraing, Belgium). For AGPase detection, an antibody raised against recombinant potato AGPase (Tiessen et al., 2002) was used. The PEPCase antibody was raised against the purified sorghum (*Sorghum vulgare*) enzyme (Vidal et al., 1983). The GWD antibody was raised against the purified protein from potato (Ritte et al., 2000a).

Analysis of Protoplast and Chloroplast Extracts

Chloroplasts were isolated from Arabidopsis protoplasts using a protocol adapted from Kunst (1998). The healthy green leaves of two mature Arabidopsis plants (approximately 4 g fresh weight) were harvested at the end of the dark period. Leaves were cut into 1-mm slices and the slices were washed for 5 min with 20 mL protoplast isolation buffer (PIB; 0.5 M sorbitol, 1 mM $CaCl_2$, 10 mM MES-KOH, pH 6.0). Cell wall digestion was done in 10 mL PIB containing degrading enzymes (100 mg cellulase Onozuka, 25 mg macerozyme Onozuka) and 100 mg polyviniylpolypyrrolidone. The slices were vacuum infiltrated and incubated without shaking at RT for 3 h. The solution was then poured over a common kitchen sieve and the digested leaf material was carefully washed drop-wise with 30 mL PIB to release the protoplasts. The protoplast suspension was passed through a nylon net with 100-μm mesh width and was then centrifuged for 5 min at 40*g* using a swing-out rotor at 4°C. The supernatant was removed with a pipette and the protoplasts were carefully resuspended in 5 mL protoplast lysis buffer (PLB; 0.4 M sorbitol, 10 mM $NaHCO_3$, 10 mM EDTA, 20 mM Tricine-KOH, pH 8.0).

For chloroplast isolation, 25 mL PLB were added to the protoplast suspension, which was hand shaken vigorously for 1 min and then passed through a nylon net with 30-μm mesh width to rupture the protoplasts. The suspension was then centrifuged at 400*g* for 2 min at 4°C and the supernatant was removed. The chloroplast pellet was carefully resuspended in 4 mL PLB. As judged by microscopic inspection, the chloroplasts were highly intact.

Three volumes of protoplast or chloroplast suspension were mixed with 1 volume of 4-fold concentrated SDS-sample buffer. Equal amounts of proteins extracted from protoplasts or chloroplasts, respectively, and M_r marker proteins were separated by SDS-PAGE (10% polyacrylamide). Western blots were performed essentially as described by Tiessen et al. (2002).

Cloning of the OK1 (PWD) cDNA

RNA was isolated from leaves of Arabidopsis wild type (ecotype Columbia) according to Logemann et al. (1987) and cDNA was prepared with the SuperScript one-step RT-PCR system (Invitrogen) using OK1rev1 primer (5′-GACTCAACCACATAACACACAAAGATC-3′). The complete OK1 coding sequence including 22 bp upstream of ATG and 69 bp downstream of TAG was amplified in a PCR reaction with the cDNA as template, the primers OK1fwd2 (5′-ATCTCTTATCACACCACCTCCAATG-3′) and OK1-rev2 (5′-TGGTAACGAGGCAAATGCAGA-3′), using the Expand High Fidelity PCR System (Roche, Mannheim, Germany). The PCR product was subcloned into a pGEM-T cloning vector (Promega, Mannheim, Germany). Sequencing of OK1pGEM-T-1 revealed an *Escherichia coli* insertion sequence (IS1) at 540 bp. Another PCR was done and a second clone (OK1pGEM-T-2) was sequenced and revealed four base substitutions compared with the published genomic sequence of At5g26570 resulting in one amino acid substitution (L854→R). A 1,081-bp *Eco*RI/*Bam*HI fragment from OK1pGEM-T-2 was replaced by the corresponding *Eco*RI/*Bam*HI fragment from OK1pGEM-T-1. Sequencing of the resulting OK1pGEM-T revealed two remaining base substitutions (G208→A; C1116→G) but no amino acid replacement.

Cloning of the OK1 (PWD) Expression Vector

The expression vector containing the OK1 coding sequence was constructed by means of the GATEWAY technology (Invitrogen) according to the manufacturer's protocols. The *att*B recombination sites were added to the OK1 cDNA in a PCR with OK1pGEM-T as template and the primers OK1EntryB1 (5′-GGGGACAAGTTTGTACAAAAAAGCAGGCTCCGAGAGCATTGGCAGCCATTG-3′) and OK1EntryB2 (5′-GGGGACCACTTTGTACAAGAAAGCTGGGTCTACAGAGGTTGTGGCCTTGAC-3′), using the Expand High Fidelity PCR System (Roche). The Entry Clone OK1pSPECTRE was obtained via the BP reaction with OK1*att*B PCR product and the Entry Clone vector pSPECTRE, which was derived from pDONR201 (Invitrogen) by replacing the *Pvu*I/*Nru*I fragment of the kanamycin resistance gene by the spectinomycin resistance gene. The OK1pDEST17 expression vector was created in the LR reaction with OK1pSPECTRE and pDEST17 (Invitrogen). Sequencing of OK1pDEST17 revealed a base transposition leading to an amino acid substitution (D143→N) in the recombinant protein.

Purification of Recombinant OK1 (PWD)

E. coli BL21 Star (DE3; Invitrogen) cells were transformed with the OK1pDEST17 plasmid and incubated in 1L TB medium containing 100 μg/mL ampicillin overnight (30°C, 250 rpm). Expression of the OK1 protein was induced by adding isopropylthio-β-galactoside to a final concentration of 1 mM at an OD_{600} of approximately 0.8. Cells were harvested at an OD_{600} of approximately 1.6 by centrifugation and stored at −80°C until use. For purification of recombinant OK1 protein cells were resuspended (0.25 g/mL) in lysis buffer (50 mM HEPES, pH 8.0, 300 mM NaCl, 10 mM imidazole, 1 mg/mL lysozyme; 1 tablet/40 mL Complete EDTA free protease inhibitors, Roche), incubated for 30 min on ice, and additionally lysed by sonification. Cell debris was removed by centrifugation and the supernatant was passed through a 0.45-μm filter. Purification of the recombinant protein was achieved using a column with 1 mL Ni-NTA agarose resin (Qiagen, Hilden, Germany). After washing with 8 mL lysis buffer, recombinant protein bound to Ni-NTA agarose was eluted with elution buffers as follows: 2 × 1 mL E1, 1 mL E2, 3 × 1 mL E3 (50 mM HEPES, pH 8.0; 300 mM NaCl; 50, 75, 250 mM imidazole for E1, E2, and E3, respectively). Fractions with adequate amount and purity of recombinant OK1 protein were pooled and concentrated by ultrafiltration (Diaflo PM30, Amicon, Millipore, Bedford, MA). The buffer in the OK1 preparation was changed using a HiTrap-Desalting column (Amersham) equilibrated with 50 mM HEPES-KOH, pH 7.5, 1 mM EDTA, 1 mM DTE. Aliquots were stored at −80°C until use.

RNAi Plants

The RNAi construct for silencing of the OK1 (PWD) gene was established by cloning a pair of short PCR-amplified OK1 cDNA fragments in opposite orientation into pHannibal (Wesley et al., 2001). The two 302-bp fragments, representing the region 2,153 to 2,454 of the complete OK1 cDNA, were obtained from PCR reactions with two primer pairs: (1) OK1-R1a-fw (5′-TCCGATGGATCCAGCAACTTCTGGTGGTCCTAT-3′) and OK1-R1a-re (5′-TTGCGCATCGATGGTCGCACTGGATTTGGAAG-3′); and (2) OK1-R1b-fw (5′-TCCGATCTCGAGACTAGTCCAGCAACTTCTGGTGGTCCT-3′) and OK1-R1b-re (5′-TTGCGCGGTACCGGTCGCACTGGATTTGGAA-3′). Appropriate restriction enzyme sites linked to the primers permitted subsequent two-step cloning of the PCR products in opposite directions into pHannibal. After digestion of the resulting vector with *Not*I restriction enzyme, the RNAi constructs were ligated into the *Not*I restriction site of the binary vector pART27 (Gleave, 1992) giving OK1-R1-pART27.

Arabidopsis plants were transformed by the dipping method of Clough and Bent (1998). Fifteen kanamycin resistant T_1 RNAi plants were analyzed by western blot for reduction of OK1 protein levels. All RNAi plants showed drastically reduced levels of OK1 protein compared with the wild type. Seeds were harvested and further analysis on starch content was done with five lines of the T_2 progeny.

Autocatalytic Phosphorylation

In vitro phosphorylation of PWD (OK1) was analyzed essentially as described for GWD (Ritte et al., 2002).

Determination of ^{33}P-Orthophosphate

A photometric assay for the detection of orthophosphate (Parvin and Smith, 1969) was modified to allow for the detection of radiolabeled orthophosphate. This assay bases on the formation of a phosphomolybdovanadate complex, followed by its subsequent extraction into butanol. In the original protocol, the maximum absorbancy of the phosphomolybdovanadate complex in butanol is measured at 310 nm against a blank, and the amount of inorganic phosphate is determined using standard curves (Parvin and Smith, 1969). Since the amounts of orthophosphate released in our enzymatic assays were too low to allow for accurate detection using the photometric assay, the activities of OK1 (PWD) or GWD were analyzed using radiolabeling assays with ^{33}P-ATP as substrate (see above) and the radioactivity in the butanol phase was determined. The activity of OK1 and GWD was tested in assays containing 10 mg starch in 0.5 mL 50 mM HEPES-KOH (pH 7.5), 1 mM EDTA, 6 mM $MgCl_2$, 0.025% Triton X-100, 10 μM ATP containing 1.65×10^6 cpm of either [γ-^{33}P]ATP or [β-^{33}P]ATP. Reactions were started by adding 20 μL (2.2 μg) of OK1 or GWD, respectively. After 80 min of incubation at RT on a rotating wheel, the samples were centrifuged (2 min, 13,000*g*) and 400 μL of the supernatant were removed and boiled for 5 min. Forty microliters of the boiled supernatant were diluted with 360 μL water. Subsequently, 800 μL butanol and 400 μL ammonium metavanadate-molybdate reagent (reagent I; Parvin and Smith, 1969) were added, the samples were mixed on a vortex for 10 s, and briefly centrifuged to achieve quick phase separation. Aliquots of the upper butanol phase (2 $\times$ 200 μL) were immediately mixed with 8 mL scintillation fluid each and the radioactivity was counted. Under the conditions applied, the recovery of inorganic phosphate in the butanol layer was $\geq$95% as determined in controls with known amounts of ^{32}P orthophosphate as internal standards. These controls are essential, as the buffer composition can substantially affect the recovery.

HPAEC-PAD Analysis

HPAEC-PAD analysis was performed essentially as described (Ritte et al., 2000b). However, a Dionex DX 600 equipped with a CarboPac PA 100 column was used. Five milligrams of in vitro phosphorylated starch were hydrolyzed with 90 μL of 0.7 N HCl for 2 h at 95°C and subsequently neutralized with 0.7 N NaOH. Prior to HPAEC-PAD analysis, samples were centrifuged through 10-kD membranes (Ultrafree MC, Millipore) that had been washed once with water.

Analysis of Starch-Bound Phosphate in Wild-Type and Transgenic Plants

All leaves from wild-type and transgenic plants (8–10 plants each) were harvested at the end of the 12-h-light period. Starch granules were isolated. Seven milligrams starch each were hydrolyzed in 150 μL 0.7 N HCl for 2 h at 95°C. Three aliquots of each granule preparation were hydrolyzed. Following neutralization and filtration through 10-kD membranes (see above), Glc was determined and samples equivalent to 5 μmol Glc each were analyzed by HPAEC-PAD. The three different hydrolyzates per starch sample yielded highly reproducible results. The elution of Glc-3-P and Glc-6-P was monitored using authentic standards.

Purification of OK1 (PWD) from Leaves of the Arabidopsis *sex1-3* Mutant

Leaves of the Arabidopsis *sex1-3* mutant were harvested at the end of the light period (20 g fresh weight), proteins were extracted, precipitated, and desalted as described. However, ammonium sulfate precipitation was from 0% to 50% saturation. Further purification was achieved by affinity chromatography using 0.5 mL maltoheptaose immobilized on agarose beads (M-9676, Sigma-Aldrich, Steinheim, Germany) in a column with gravity flow. All steps were carried out at 4°C. The column was washed with 10 mL binding buffer, 2.5 mL protein extract (19.5 mg protein) was applied, and the flowthrough was applied once more. After washing with 10 mL binding buffer, bound proteins were eluted with Dextri maltose (ICN, Eschwege, Germany) dissolved in binding buffer (1 mL 10 mg/mL followed by 1 mL 50 mg/mL). Eluted proteins were further concentrated using spin column filters with an exclusion limit of 10 kD (Amicon YM-10,Microcon, Millipore), washed with 1 volume binding buffer, and again concentrated 4-fold with spin columns to give a final volume of 0.5 mL with a protein concentration of 50 μg/mL.

Analysis of Starch Content in Leaves

Measuring of the leaf starch content was done basically as described by Abel et al. (1996). All leaves of 4- to 5-week-old plants were harvested, frozen in liquid nitrogen, and homogenized in a mortar. Samples of 40 to 60 mg homogenized material were extracted 2 times, each with 1 mL 80% (v/v) ethanol for 20 min at 80°C. Insoluble material was washed in 1 mL water, vacuum dried, resuspended in 0.5 mL 0.2 N KOH, and incubated at 95°C or 1 h. After neutralization with 1 N acetic acid and centrifugation, 25 μL of the supernatant were mixed with 50 μL amyloglucosidase solution (starch determination kit, R-Biopharm, Darmstadt, Germany). However, we supplemented the amyloglucosidase solution with 1 unit of α-amylase from *Bacillus amyloliquefaciens* (Roche). Enzymatic hydrolysis of starch and subsequent enzymatic determination of Glc was performed according to the provider's protocol.

Upon request, all novel materials described in this publication will be made available in a timely manner for noncommercial research purposes, subject to the requisite permission from any third-party owners of all or parts of the material. Obtaining any permissions will be the responsibility of the requestor.

Sequence data from this article have been deposited with the EMBL/GenBank data libraries under accession number AJ635427.

ACKNOWLEDGMENTS

We thank Anja Fröhlich and Torsten Schulze (MPI, Golm, Germany) for helping with plant transformation, Silke Gopp for the maintenance of plants, Anke Scharf for technical assistance, and Nora Eckermann (Plant Physiology, University of Potsdam, Germany) for advice in the HPAEC-PAD analysis. We are grateful to Jean Vidal (University of Paris) and Maria Ines Zanor (MPI) for the gift of the anti-PEPcarboxylase antibody, and Ben Trevaskis (Commonwealth Scientific and Industrial Research Organization, Canberra, Australia) for the gift of pSPECTRE vector plasmid. We thank the Salk Institute and the Nottingham Arabidopsis Stock Center for provision of the T-DNA insertion line.

Received November 3, 2004; returned for revision November 16, 2004; accepted November 16, 2004.

LITERATURE CITED

Abel GJ, Springer F, Willmitzer L, Kossmann J (1996) Cloning and functional analysis of a cDNA encoding a novel 139 kDa starch synthase from potato (*Solanum tuberosum* L.). Plant J **10:** 981–991

Blennow A, Bay-Smidt AM, Olsen CE, Møller BL (1998) Analysis of starch-bound glucose 3-phosphate and glucose 6-phosphate using controlled acid treatment combined with high-performance anion-exchange chromatography. J Chromatogr A **829:** 385–391

Blennow A, Nielsen TH, Baunsgaard L, Mikkelsen R, Engelsen SB (2002) Starch phosphorylation: a new front line in starch research. Trends Plant Sci **7:** 445–450

Clough SJ, Bent AF (1998) Floral dip: a simplified method for *Agrobacterium*-mediated transformation of *Arabidopsis thaliana*. Plant J **16:** 735–743

Dong Q, Schlueter SD, Brendel V (2004) PlantGDB, plant genome database and analysis tools. Nucleic Acids Res **32:** D354–D359

Emanuelsson O, Nielsen H, Brunak S, von Heijne G (2000) Predicting subcellular localization of proteins based on their N-terminal amino acid sequence. J Mol Biol **300:** 1005–1016

Engelsen SB, Madsen AO, Blennow A, Motawia MS, Møller BL, Larsen S (2003) The phosphorylation site in double helical amylopectin as investigated by a combined approach using chemical synthesis, crystallography and molecular modeling. FEBS Lett **541:** 137–144

Gleave AP (1992) A versatile binary vector system with a T-DNA organisational structure conducive to efficient integration of cloned DNA into the plant genome. Plant Mol Biol **20:** 1203–1207

Goss NH, Evans CT, Wood HG (1980) Pyruvate phosphate dikinase: sequence of the histidyl peptide, the pyrophosphoryl and phosphoryl carrier. Biochemistry **19:** 5805–5809

Kleffmann T, Russenberger D, von Zychlinski A, Christopher W, Sjölander K, Gruissem W, Baginsky S (2004) The *Arabidopsis thaliana* chloroplast proteome reveals pathway abundance and novel protein functions. Curr Biol **14:** 354–362

Kokesh FC, Cameron DA, Kakuda Y, Kuras PV (1978) Hydrolysis of alpha-D-glucopyranose 1,2-cyclic phosphate: the effect of pH and temperature on product distribution, and position of opening of phosphate diester ring in formation of D-glucose 2-phosphate. Carbohydr Res **62:** 289–300

Kunst L (1998) Preparation of physiologically active chloroplasts from Arabidopsis. Methods Mol Biol **82:** 43–48

Logemann J, Schell J, Willmitzer L (1987) Improved method for the isolation of RNA from plant tissues. Anal Biochem **163:** 16–20

Lorberth R, Ritte G, Willmitzer L, Kossmann J (1998) Inhibition of a starch-granule-bound protein leads to modified starch and repression of cold sweetening. Nat Biotechnol **16:** 473–477

Marchler-Bauer A, Anderson JB, DeWeese-Scott C, Fedorova ND, Geer LY, He S, Hurwitz DI, Jackson JD, Jacobs AR, Lanczycki CJ, et al (2003) CDD: a curated Entrez database of conserved domain alignments. Nucleic Acids Res **31:** 383–387

Mikkelsen R, Baunsgaard L, Blennow A (2004) Functional characterization of alpha-glucan,water dikinase, the starch phosphorylating enzyme. Biochem J **377:** 525–532

Narindrasorasak S, Bridger WA (1977) Phosphoenolypyruvate synthetase of *Escherichia coli*: molecular weight, subunit composition, and identification of phosphohistidine in phosphoenzyme intermediate. J Biol Chem **252:** 3121–3127

Nielsen TH, Wischmann B, Enevoldsen K, Møller BL (1994) Starch phosphorylation in potato tubers proceeds concurrently with de novo biosynthesis of starch. Plant Physiol **105:** 111–117

Parvin R, Smith RA (1969) Determination of inorganic phosphate in the presence of labile organic phosphates. Anal Biochem **27:** 65–72

Reimann R, Hippler M, Machelett B, Appenroth KJ (2004) Light induces phosphorylation of glucan water dikinase, which precedes starch degradation in turions of the duckweed *Spirodela polyrhiza*. Plant Physiol **135:** 121–128

Ritte G, Eckermann N, Haebel S, Lorberth R, Steup M (2000b) Compartmentation of the starch-related R1 protein in higher plants. Starch-Stärke **52:** 179–185

Ritte G, Lloyd JR, Eckermann N, Rottmann A, Kossmann J, Steup M (2002) The starch-related R1 protein is an alpha-glucan, water dikinase. Proc Natl Acad Sci USA **99:** 7166–7171

Ritte G, Lorberth R, Steup M (2000a) Reversible binding of the starch-related R1 protein to the surface of transitory starch granules. Plant J **21:** 387–391

Ritte G, Scharf A, Eckermann N, Haebel S, Steup M (2004) Phosphorylation of transitory starch is increased during degradation. Plant Physiol **135:** 2068–2077

Ritte G, Steup M, Kossmann J, Lloyd JR (2003) Determination of the starch-phosphorylating enzyme activity in plant extracts. Planta **216:** 798–801

Rosenberg IM (1996) Modified proteins and peptides. B. Phosphorylation. *In* IM Rosenberg, ed, Protein Analysis and Purification: Benchtop Techniques. Birkhäuser, Boston, pp 224–244

Slattery CJ, Kavakli IH, Okita TW (2000) Engineering starch for increased quantity and quality. Trends Plant Sci **5:** 291–298

Tabata S, Hizukuri S (1971) Studies on starch phosphate. 2. Isolation of glucose 3-phosphate and maltose phosphate by acid hydrolysis of potato starch. Starch-Stärke **23:** 267–272

Tatusova TA, Madden TL (1999) BLAST 2 Sequences, a new tool for comparing protein and nucleotide sequences. FEMS Microbiol Lett **174:** 247–250

Tiessen A, Hendriks JH, Stitt M, Branscheid A, Gibon Y, Farré EM, Geigenberger P (2002) Starch synthesis in potato tubers is regulated by post-translational redox modification of ADP-glucose pyrophosphorylase: a novel regulatory mechanism linking starch synthesis to the sucrose supply. Plant Cell **14:** 2191–2213

Vidal J, Godbillon G, Gadal P (1983) Influence of light on phosphoenol pyruvate-carboxylase in sorghum leaves. 2. Immunochemical study. Physiol Plant **57:** 124–128

Wesley SV, Helliwell CA, Smith NA, Wang MB, Rouse DT, Liu Q, Gooding PS, Singh SP, Abbott D, Stoutjesdijk PA, et al (2001) Construct design for efficient, effective and high-throughput gene silencing in plants. Plant J **27:** 581–590

Wischmann B, Nielsen TH, Møller BL (1999) In vitro biosynthesis of phosphorylated starch in intact potato amyloplasts. Plant Physiol **119:** 455–462

Yu TS, Kofler H, Häusler RE, Hille D, Flügge UI, Zeeman SC, Smith AM, Kossmann J, Lloyd J, Ritte G, et al (2001) The Arabidopsis *sex1* mutant is defective in the R1 protein, a general regulator of starch degradation in plants, and not in the chloroplast hexose transporter. Plant Cell **13:** 1907–1918

Zeeman SC, Smith SM, Smith AM (2004) The breakdown of starch in leaves. New Phytol **163:** 247–261

Exhibit C

Journal of Experimental Botany, Vol. 58, No. 14, pp. 3949–3960, 2007
doi:10.1093/jxb/erm249 Advance Access publication 17 November, 2007
This paper is available online free of all access charges (see http://jxb.oxfordjournals.org/open_access.html for further details)

Journal of Experimental Botany
www.jxb.oxfordjournals.org

RESEARCH PAPER

An extra-plastidial α-glucan, water dikinase from *Arabidopsis* phosphorylates amylopectin *in vitro* and is not necessary for transient starch degradation

Mikkel A. Glaring[1,*], Agnieszka Zygadlo[1,†], David Thorneycroft[3], Alexander Schulz[2], Steven M. Smith[3,4], Andreas Blennow[1] and Lone Baunsgaard[1,†]

[1] *Plant Biochemistry Laboratory, Center for Molecular Plant Physiology (PlaCe), Department of Plant Biology, Faculty of Life Sciences, University of Copenhagen, 40 Thorvaldsensvej, 1871 Frederiksberg C, Copenhagen, Denmark*

[2] *Plant Physiology and Anatomy Laboratory, Department of Plant Biology, Faculty of Life Sciences, University of Copenhagen, Denmark*

[3] *Institute of Molecular Plant Sciences, University of Edinburgh, Edinburgh EH9 3JH, UK*

[4] *ARC Centre of Excellence in Plant Energy Biology, University of Western Australia, WA 6009, Australia*

Received 18 July 2007; Revised 17 September 2007; Accepted 18 September 2007

Abstract

Starch phosphorylation catalysed by the α-glucan, water dikinases (GWD) has profound effects on starch degradation in plants. The *Arabidopsis thaliana* genome encodes three isoforms of GWD, two of which are localized in the chloroplast and are involved in the degradation of transient starch. The third isoform, termed AtGWD2 (At4g24450), was heterologously expressed and purified and shown to have a substrate preference similar to potato GWD. Analyses of *AtGWD2* null mutants did not reveal any differences in growth or starch and sugar levels, when compared to the wild type. Subcellular localization studies in *Arabidopsis* leaves and *in vitro* chloroplast import assays indicated that AtGWD2 was not targeted to the chloroplasts. The *AtGWD2* promoter showed a highly restricted pattern of activity, both spatially and temporally. High activity was observed in the companion cells of the phloem, with expression appearing just before the onset of senescence. Taken together, these data indicate that, although AtGWD2 is capable of phosphorylating α-glucans *in vitro*, it is not directly involved in transient starch degradation.

Key words: *Arabidopsis*, dikinase, GWD, phloem, starch degradation, starch phosphorylation.

Introduction

In recent years, significant progress has been made in elucidating the enzymatic pathways responsible for the degradation of transient starch in *Arabidopsis thaliana* (Lloyd *et al.*, 2005; Smith *et al.*, 2005; Zeeman *et al.*, 2007). Analysis of plants mutated in plastidic glucan phosphorylase has suggested that the phosphorolytic pathway of starch degradation is not required under normal growth conditions (Zeeman *et al.*, 2004). Rather, hydrolytic breakdown of starch leads to the formation of maltose and glucose as primary products of degradation (Niittylä *et al.*, 2004; Weise *et al.*, 2004). The analysis of starch degradation is confounded by the multitude of isoforms of enzymes capable of degrading starch or related glucans. Few studies of starch metabolism in *Arabidopsis* have focused on the function of starch-degrading enzymes not directly involved in the metabolism of transient starch or its degradation products. Many of these enzymes show subcellular localizations not compatible with a plastidic localization of starch and suggest alternative locations of starch or starch-like molecules. The *Arabidopsis* genome encodes two α-amylases and six β-amylases predicted to be localized outside the plastids (Lloyd *et al.*, 2005). No *in vivo* substrate has so far been identified for any of these enzymes and there is little experimentally based information on their subcellular

* To whom correspondence should be addressed. E-mail: mig@life.ku.dk
† Present address: Aresa A/S, Symbion Science Park, 3 Fruebjergvej, 2100 Copenhagen Ø, Denmark.

localization. Mutations in the extra-plastidial isoform of β-amylase RAM1 (BAM5), which has been localized to the phloem (Wang *et al.*, 1995), lead to a significant decrease in β-amylase activity in *Arabidopsis*, but only minor changes in starch metabolism (Laby *et al.*, 2001; Kaplan and Guy, 2005).

The enzyme responsible for the initial attack on the granule has not been clearly identified, but contrary to previous beliefs, it has been determined that the endoamylolytic action of α-amylases is not solely responsible for this process (Kaplan and Guy, 2005; Yu *et al.*, 2005). The production of maltose during the degradation of starch has implicated the β-amylases in starch degradation. β-amylases are exoamylases that produce maltose by successive cleavage from the non-reducing end. Furthermore, a recent report has provided evidence that the debranching enzyme (isoamylase) ISA3 acts directly at the granule surface in *Arabidopsis* (Delatte *et al.*, 2006). This debranching activity presumably removes short branches from the granule surface enabling further degradation by the β-amylases. Based on these results, it was suggested that ISA3 and β-amylase act progressively to degrade the starch granule surface (Delatte *et al.*, 2006). Suppression of a chloroplast-localized β-amylase in *Arabidopsis* (BAM3), and the corresponding potato orthologue, leads to a starch-excess phenotype in leaves as a result of impaired starch degradation (Scheidig *et al.*, 2002; Kaplan and Guy, 2005). Maltose produced by β-amylase is exported from the chloroplast by the transporter MEX1 (Niittylä *et al.*, 2004) and further metabolized in the cytosol by the glucanotransferase DPE2 (Chia *et al.*, 2004; Lu and Sharkey, 2004). This process involves a recently identified cytosolic soluble heteroglycan (Fettke *et al.*, 2005). This heteroglycan has been studied in *DPE2* mutants and found to be indirectly involved in starch degradation partly by acting as a carbohydrate acceptor for the DPE2-catalysed transfer of glucose from maltose (Fettke *et al.*, 2006).

Regardless of the mechanism of soluble glucan release from the starch granule, it is clear that it requires the activity of the α-glucan, water dikinases (GWD, Lorberth *et al.*, 1998; Yu *et al.*, 2001; Ritte *et al.*, 2002). The GWDs are responsible for phosphorylating the glycosyl residues of starch, a process that takes place during both biosynthesis and degradation (Nielsen *et al.*, 1994; Ritte *et al.*, 2004). Repressing or eliminating the activity of potato GWD or the *Arabidopsis* orthologue AtGWD1/SEX1 (At1g10760), leads to a severely reduced phosphate content in starch and a starch-excess phenotype in leaves caused by a decreased rate of starch degradation (Lorberth *et al.*, 1998; Yu *et al.*, 2001). One homologue of AtGWD1 in *Arabidopsis*, termed AtGWD3 or PWD (At5g26570), is chloroplastic and involved in the phosphorylation of pre-phosphorylated glucans, an activity which is essential for the complete degradation of transient starch during the night (Baunsgaard *et al.*, 2005; Kötting *et al.*, 2005). Despite the essential role of starch-bound phosphate in starch degradation, the link between phosphorylation and degradation is not understood. It has been suggested that the activity of amylolytic enzymes might rely on direct interaction with phosphate groups or that the inclusion of phosphate affects the properties of amylopectin (Blennow *et al.*, 2002; Ritte *et al.*, 2002). A recent report has shown that GWD activity stimulates the breakdown of starch granules *in vitro* by plastidial β-amylases, leading the authors to suggest that phosphorylation by GWD causes a partial unwinding of the amylopectin double helix, thereby facilitating a subsequent enzymatic attack (Edner *et al.*, 2007).

A third GWD, named AtGWD2, with 50% homology to AtGWD1 has been identified in the *Arabidopsis* genome (Yu *et al.*, 2001). AtGWD2 has a domain structure more similar to AtGWD1 than AtGWD3/PWD, but lacks an apparent chloroplast transit peptide, making it likely to be a cytosolic isoform of GWD. The putative extra-plastidial glucan phosphorylating activity raises some interesting questions about the function of AtGWD2 and prompted us to investigate the substrate preference of this enzyme and its involvement in transient starch metabolism.

Materials and methods

Plant material and growth conditions

The mutant *Atgwd2-1* was obtained by screening a T-DNA transformed *Arabidopsis* population from the University of Wisconsin Arabidopsis knockout facility (Krysan *et al.*, 1999). *Atgwd2-2* was obtained directly from the GABI-Kat program (line 257E09; www.gabi-kat.de; Rosso *et al.*, 2003). The mutant *Atgwd2-3* was obtained from the SALK T-DNA mutant population (line SALK_080260; Alonso *et al.*, 2003) provided by the European *Arabidopsis* Stock Centre (NASC, http://arabidopsis.info). Homozygous mutants were isolated by PCR screening of isolated genomic DNA. Standard PCR conditions were used to amplify a section of DNA spanning the reported insertion site in *AtGWD2* (insert test primers for *Atgwd2-1*; GWDb3: AGAACTCTCCAAGAGATCTGTGGGC, GWDb4r: ATCTCTCAGCCTCTTTCTCTCGCTC, *Atgwd2-2*; GWDb10: GAGACTAACTATGGCACTTGTGGGT, GWDb11r: CCATTGACAGCAAAGACATGATGACC, *Atgwd2-3*; GWDb1: TACAGACCTCATGATGTTCAGTGGG, GWD2-12r: GATATTGCTCTCCCTTCCTTCGACT). Positives were verified by PCR using the insert test primers and primers matching the T-DNA border. Total RNA was isolated and reverse transcribed using standard molecular biology methods. The absence of a functional *AtGWD2* transcript was verified by PCR using the insert test primers and a positive control. The *Arabidopsis thaliana* ecotypes Columbia-0 and Wassilewskija and the *Atgwd2* mutants were grown from seed in potting compost in growth chambers at 20 °C and 70% relative humidity with an 8 h photoperiod at a photon flux density of 120 μmol photons m^{-2} s^{-1}.

Phylogenetic analysis

The phylogenetic tree was based on a previous version containing GWD sequences identified from higher plants (Baunsgaard *et al.*, 2005). This tree was based on the alignment of the nucleotide

binding domains corresponding to amino acids 1006–1194 of AtGWD3. The tree was expanded by the addition of a new citrus homologue of AtGWD2 identified in HarvEST (unigene #16433, http://harvest.ucr.edu) and two pairs of poplar sequences of which one from each pair is represented in the phylogenetic tree (GWD3 clade: genome scaffold LG_II: 22.012.650-22.013.216 and GWD1 clade: LG_VIII: 12.855.187-12.856.452; http://www.jgi.doe.gov/poplar). Furthermore, sequences from organisms other than higher plants were included in the analysis. Three GWD homologues from the green alga *Chlamydomonas reinhardtii* were identified from a previously published phylogenetic analysis of GWDs [Mikkelsen *et al.*, 2004; accession nos *Chlamydomonas* a, BG857380; b, BF866067/AW661031; c, genome release version 3.0, scaffold 32, 64268–65561 (http://genome.jgi-psf.org/Chlre3)]. Two GWDs from the green alga *Ostreococcus tauri* were identified in GenBank [accession nos AY570708 (spr1a) and AY570720 (spr1b)]. GWD homologues from the apicomplexan parasites *Cryptosporidium parvum* (mRNA sequence, accession no. XM_626438) and *Toxoplasma gondii* (assembled from EST accession nos BU575407, BG658300, BG659286, CN194874, and genomic sequence) were also included. Other accession numbers were as follows. AtGWD1 clade: AtGWD1, NP_563877; rice, AK103463; maize, AY109804; wheat, CAC22583; barley, BU993123; citrus, AAM18228; grape, EE077235; potato, Q9AWA5; tomato, BE435569; soybean, AW133227/BI945390; *Medicago*, CAE84830. AtGWD2 clade: AtGWD2, AAO42141. AtGWD3 clade: AtGWD3, AY747068; maize, AY108492; rice, AK072331; *Medicago*, BM779840. The alignment and the phylogenetic tree were created using the MEGA3 software available at www.megasoftware.net (Kumar *et al.*, 2004).

Glucan-bound phosphate content

Glucose-6-phosphate and glucose-3-phosphate contents were determined by acid hydrolysis of glucan substrates followed by high-performance anion-exchange chromatography with pulsed amperometric detection (HPAEC-PAD) as previously described (Blennow *et al.*, 1998). To minimize interference from incompletely hydrolysed glucans, samples were hydrolysed for 4 h. This minimizes, but does not eliminate, the content of maltose-6-phosphate which co-elutes with glucose-3-phosphate under the conditions used (Ritte *et al.*, 2006). For the determination of C-6 to C-3 phosphorylation ratios, 0.5 ml fractions were collected and the incorporated label was measured by a liquid scintillation counter (1450 Microbeta, Perkin-Elmer).

Expression, purification and substrate specificity of AtGWD2

AtGWD2 was expressed in *Saccharomyces cerevisiae* as a C-terminal fusion to a V5 epitope and polyhistidine tag (6×His) and purified by affinity chromatography as previously described by Baunsgaard *et al.* (2005). The *waxy* maize amylopectin substrates were generated as described by Baunsgaard *et al.* (2005). Soluble starch from potato was obtained from Sigma-Aldrich (product number S 2004).

Autocatalytic phosphorylation and dikinase assays

For the determination of autocatalytic phosphorylation (autophosphorylation), a 10 μg sample of purified AtGWD2 was analysed as described by Mikkelsen *et al.* (2004). Dikinase activity assays were performed essentially as previously described by Mikkelsen *et al.* (2004). One microgram of purified AtGWD2 was incubated with 10 μM [β-^{33}P]ATP (150 000 dpm) and 5 mg ml^{-1} glucan substrate in a final volume of 100 μl (25 mM HEPES/KOH, pH 7.0, 10 mM NH_4Cl, 10 mM $MgCl_2$, 0.5 mM DTT, 0.2 mg ml^{-1} BSA). The reaction was incubated for 1 h at 30 °C and terminated by boiling. The polyglucan was precipitated with 1.8 ml 75% methanol/1% KCl and resuspended in 200 μl of water. This procedure was repeated four times and the final pellet was dissolved in 400 μl of water. Incorporation of labelled phosphate was determined by adding 3 ml scintillation liquid to the mixture and measuring the radioactivity with a liquid scintillation counter (1450 Microbeta, Perkin-Elmer). Initial enzyme kinetic studies using soluble potato starch as a substrate confirmed that the rate of phosphate incorporation was constant over the entire assay period and increased linearly with respect to enzyme concentration.

Expression analysis

For analysis of *AtGWD2* expression, a 1207 bp promoter fragment (primers GWDb1: 5' GAT GCA AAT TGT CTG CAG GGA AT; GWDFL: 5' GGC AGC TAT TCA TAA AAA AGA GGT AAC A, including an *attB1* and *attB2* site, respectively) was cloned in front of an enhanced green fluorescent protein (eGFP)-β-glucoronidase (GUS) fusion in the vector pKGWFS7 (Karimi *et al.*, 2002) using the GATEWAY™ cloning technology (Invitrogen). The construct was transformed into *Agrobacterium* and introduced into *Arabidopsis thaliana* ecotype Columbia-0. After an initial screening of transgenic lines in the T_1 and T_2 generations, five lines were chosen for detailed analysis. GUS activity was determined by harvesting plant parts directly into an X-Gluc solution [1 mg ml^{-1} 5-bromo-4-chloro-3-indolyl β-D-glucuronide cyclohexylammonium salt (Duchefa Biochemie, The Netherlands), 10 mM titriplex III, 2 mM $K_3[Fe(CN)_6]$ and 2 mM $K_4[Fe(CN)_6]$ in a 0.1 M phosphate buffer pH 7.5], vacuum infiltrating for 30 min and incubating at 37 °C for 24 h. Stained material was subjected to a 20–50% ethanol series, fixed in FAA (50% ethanol, 5% formaldehyde, 10% acetic acid) for 30 min and subsequently destained with 70% ethanol before microscopy analysis.

GFP activity was investigated by confocal laser scanning microscopy as previously described by Baunsgaard *et al.* (2005). Staining for sieve-plates was performed by incubating thin strips of mature *Arabidopsis* leaves in a solution of analine blue for 30 min, followed by immediate inspection by confocal laser scanning microscopy (TCS SP2; Leica Microsystems, Wetzlar, Germany). A two-photon laser operating at 800 nm was used for excitation and emission was detected in the interval between 450 nm and 510 nm.

Subcellular localization

The entire ORF of AtGWD2 as well as a fragment containing the 158 N-terminal amino acids was fused to enhanced GFP (eGFP) behind the constitutive 35S promoter in the binary vector pK7FWG2 (Karimi *et al.*, 2002) using the GATEWAY™ cloning technology (Invitrogen). The constructs were introduced into *Arabidopsis thaliana* ecotype Columbia-0. For tobacco transient expression, fragments of AtGWD2 were PCR amplified using uracil-containing primers and cloned into the vector pPS48uYFP using an improved USER™ (uracil-specific excision reagent, New England Biolabs) cloning procedure (Nour-Eldin *et al.*, 2006). The transit peptide of AtGWD1 was fused to AtGWD2 by simultaneous cloning of both fragments. The constructs were transformed into *Agrobacterium* and transiently expressed by infiltration in *Nicotiana benthamiana* as previously described by Voinnet *et al.* (2003). All constructs were analysed by a confocal laser scanning microscope (TCS SP2; Leica Microsystems, Wetzlar, Germany) equipped with a 20×/0.70 or 63×/1.20 PL APO water immersion objective. A 488 nm laser line was used for excitation and emission was detected between 510 nm and 535 nm for GFP fluorescence, 520 nm and 550 nm for YFP fluorescence, and 650 nm and 750 nm for chlorophyll autofluorescence.

In vitro *import assays*

Constructs containing *AtGWD2* alone and *AtGWD2* fused to the predicted transit peptide of *AtGWD1* were cloned in the vector

pGEM-4Z (Promega GmbH, Mannheim, Germany) and transcribed *in vitro* using SP6 RNA polymerase. Products were translated *in vitro* in the presence of [^{3}H]leucine using a Rabbit Reticulocyte Lysate system (Promega GmbH, Mannheim, Germany) according to the manufacturer's instructions. Intact chloroplasts were isolated from pea seedlings (*Pisum sativum*, var. Kelvedon Wonder) and *in vitro* import assays were carried out as reported by Robinson and Mant (2002). Samples were analysed by SDS-PAGE and autoradiography.

Electron microscopy

Inflorescence segments were cut from *Arabidopsis* wild-type Columbia-0 and the mutant *Atgwd2-2*. Fixation, staining, and image acquisition was performed as previously described by Schulz *et al.* (1998).

Results

The AtGWD2 homologue

A cDNA encoding AtGWD2 was obtained from the RIKEN *Arabidopsis* full-length (RAFL) cDNA collection (GenBank accession no. BT004118). This clone included the entire 1278 amino acids open reading frame (ORF) plus 5' and 3' untranslated regions. It is encoded by a 7.4 kb locus on chromosome 4 divided into 32 exons (At4g24450). The ORF includes the conserved phosphohistidine and nucleotide binding domains in the C-terminal end and the tandem repeated starch binding domains in the N-terminal end, similar to those present in AtGWD1 and potato GWD (Yu *et al.*, 2001; Mikkelsen *et al.*, 2006). The starch binding domain from potato GWD has been shown to bind to granular starch *in vitro* and this type of domain appears to be specific for enzymes involved in plastidial starch metabolism (Mikkelsen *et al.*, 2006). Alignment of the conserved tryptophanes in the starch binding domains (Mikkelsen *et al.*, 2006) showed that AtGWD2 lacks 78 amino acids in the N-terminal, when compared to AtGWD1. This truncation covers the entire predicted transit peptide of AtGWD1. Prediction of putative subcellular location by Predotar (http://urgi.versailles.inra.fr/predotar; Small *et al.*, 2004) and TargetP (www.cbs.dtu.dk/services/TargetP; Emanuelsson *et al.*, 2000) did not indicate the presence of a transit peptide. Together these observations suggest that AtGWD2 is a non-plastidic paralogue of AtGWD1.

Available sequence databases were analysed in an effort to identify putative orthologues of *AtGWD2* in other plants. Numerous homologous sequences were identified among ESTs and genomic survey sequences from *Brassica napus*, *Brassica rapa*, and *Brassica oleracea*, although none of these sequences (either singly or assembled) covered the entire nucleotide binding domain used in previous phylogenetic studies of GWDs (Baunsgaard *et al.*, 2005). The sequence identity to *AtGWD2* was generally high, usually around 70–90% at both the nucleotide and protein levels depending on the sequence region. An EST clone from the bark of *Poncirus trifoliata* was identified in GenBank (accession nos CV711759 and CV711760). The clone belongs to a unigene cluster assembled from four sequences from *Poncirus trifoliata* (2), *Citrus clementina* (1), and *Citrus sinensis* (1) in the HarvEST project (http://harvest.ucr.edu). The sequence matches the 475 C-terminal amino acids of AtGWD2 and shows 68% identity and 82% similarity at the protein level. Intriguingly, this clone is the only indication of the existence of GWD2 orthologues outside the Brassicaceae family, to which *Arabidopsis* belongs. The poplar genome contained four GWD homologues, represented as pairs of closely related sequences, but no homologues of *AtGWD2*. A search of the rice genome revealed two sequences similar to *AtGWD1* and *AtGWD3/PWD* from *Arabidopsis*. No sequence with significant homology to *AtGWD2* was present, indicating that the monocot rice does not contain this isoform.

The phylogenetic study of higher plant GWDs previously reported (Baunsgaard *et al.*, 2005) was expanded by including newly identified sequences from higher plants, the apicomplexan parasites *Cryptosporidium parvum* and *Toxoplasma gondii* and sequences from the green algae *Chlamydomonas reinhardtii* and *Ostreococcus tauri*. The phylogenetic tree showed two groups of GWDs comprising the orthologues of AtGWD1 and AtGWD3/PWD from higher plants (Fig. 1). The two representatives of GWD2 formed a group closely related to the GWD1 sequences, clearly demonstrating their relationship with the GWD1 group.

Expression and purification of AtGWD2

A fusion protein consisting of AtGWD2 and a C-terminal V5 epitope and polyhistidine tag (6×His) was heterologously expressed in *Saccharomyces cerevisiae* and purified to apparent homogeneity using affinity chromatography. The identity of the fusion protein was confirmed by SDS-PAGE and immunoblotting using an anti-V5 antibody. Enzyme activity was verified by autophosphorylation of the purified protein following incubation with [β-^{33}P]ATP. Autophosphorylation is the first step in the dikinase reaction mechanism. It results in a stable phosphorylated intermediate and the step can be completed in the absence of a glucan substrate (Ritte *et al.*, 2002; Mikkelsen *et al.*, 2004). Separation of the labelled products by SDS-PAGE and visualization by autoradiography revealed that AtGWD2 was significantly labelled by this procedure (Fig. 2).

Substrate specificity of AtGWD2

The *in vitro* substrate specificity of purified AtGWD2 was investigated using a series of enzymatically modified substrates previously used to characterize the AtGWD3 enzyme (Baunsgaard *et al.*, 2005). These substrates were

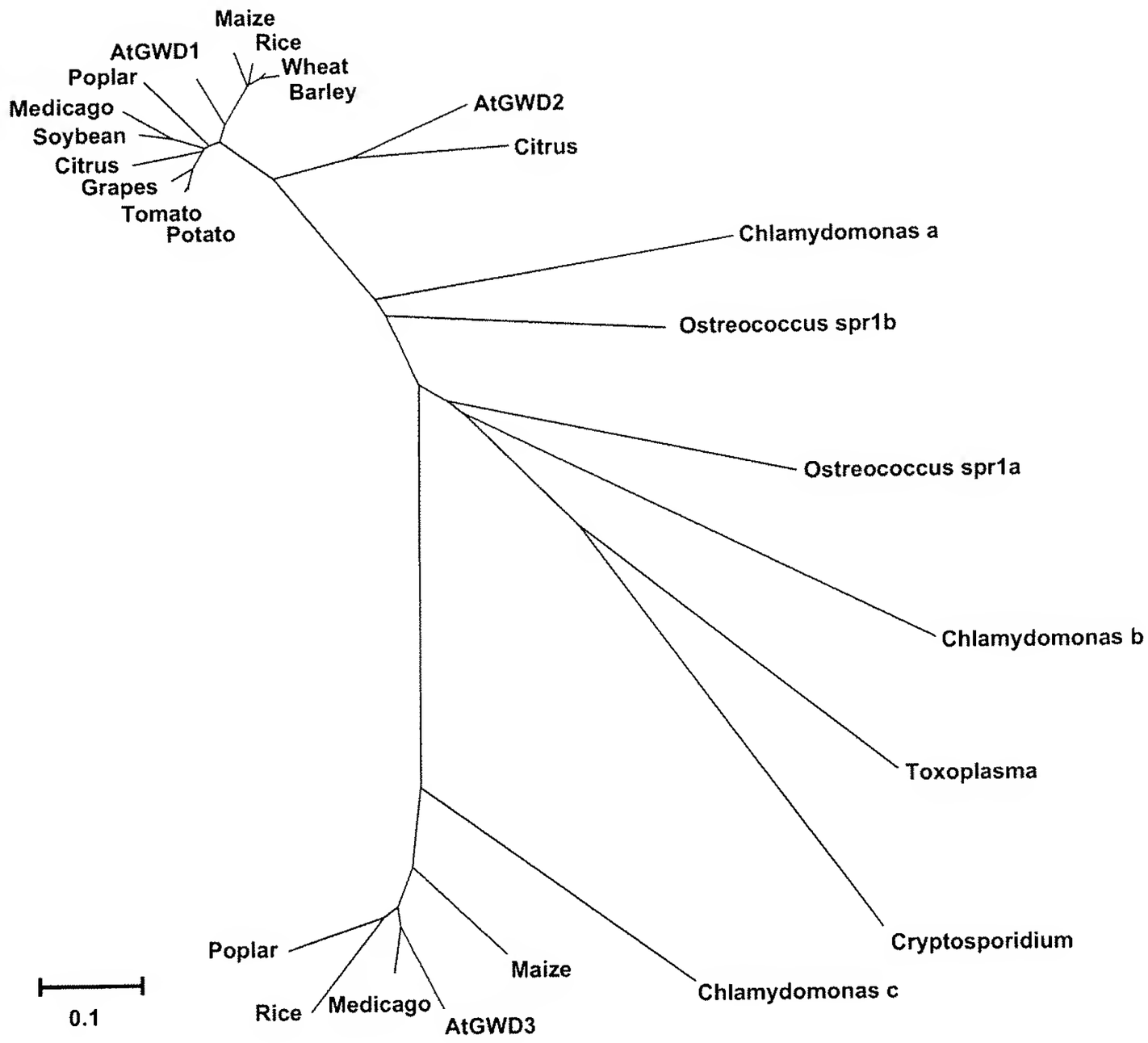

Fig. 1. A phylogenetic tree of the nucleotide binding domain of GWD sequences from selected organisms. The tree was constructed on the basis of available protein sequences or translated genome sequences and expressed sequence tags. The alignment was created and visualized using the MEGA3 software (Kumar *et al.*, 2004). Accession numbers are given in the Materials and methods. The scale indicates the average substitutions per site.

based on *waxy* maize amylopectin, which has a very low natural level of covalently linked phosphate-groups. Three modified substrates were generated: (i) *waxy* maize amylopectin elongated by phosphorylase *a*, (ii) *waxy* maize amylopectin pre-phosphorylated with purified potato GWD, and (iii) elongated and pre-phosphorylated *waxy* maize amylopectin. Purified AtGWD2 was incubated with [β-^{33}P]ATP and the maize glucan substrates and the efficiency of glucan phosphorylation was determined by measuring the amount of incorporated label (Table 1). Minimal activity was detected on glycogen (data not shown), the unmodified amylopectin, and the pre-phosphorylated amylopectin. Elongating the amylopectin substrate led to a large increase in specific activity and pre-phosphorylation further increased this activity. Maximum activity was obtained on a soluble starch from potato. Soluble potato starch has previously been used as a substrate for determining starch-phosphorylating enzyme activity in plant extracts (Ritte *et al.*, 2003). The substrate specificity of AtGWD2 thus resembles the results obtained for potato GWD (Ritte *et al.*, 2002; Mikkelsen *et al.*, 2004) and the activity is not dependent on previous

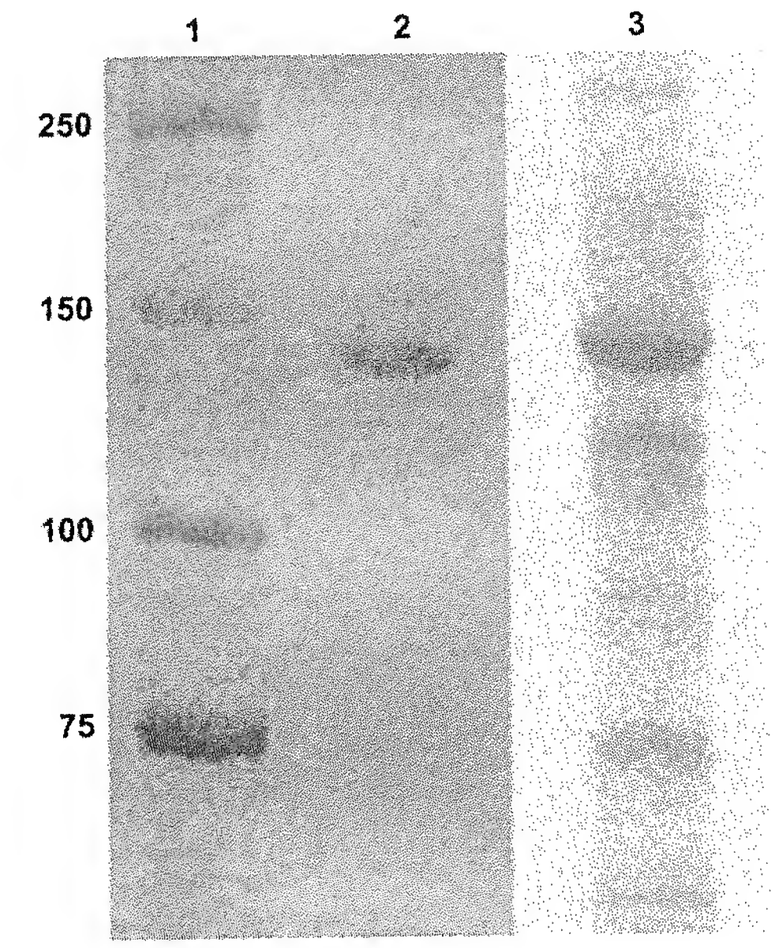

Fig. 2. Autophosphorylation of purified AtGWD2. (1) Marker. (2) Purified AtGWD2 incubated with [β-^{33}P]ATP, separated by SDS-PAGE and stained with Coomassie Brilliant Blue. (3) Autoradiogram of lane 2.

Table 1. *Activity of purified AtGWD2 on various glucan substrates*

Substrate	Mean chain length (DP)[c]	Phosphate content[a, c]	Specific activity (mU mg^{-1} protein)[b]
Amylopectin	23.5	0.1	0.02±0.01
Amylopectin, pre-phosphorylated	24.8	0.5	0.04±0.01
Amylopectin, elongated	29.7	0.1	0.49±0.02
Amylopectin, elongated and pre-phosphorylated	30.8	39.4	0.65±0.18
Soluble starch	ND	ND	1.36±0.21

[a] nmol glucose-6-phosphate mg^{-1} starch.
[b] 1 unit (U) is defined as 1 μmol phosphate incorporated min^{-1} at 30 °C.
[c] Values for mean chain length and glucose-6-phosphate content were obtained from Baunsgaard *et al.* (2005). Standard deviations from three activity experiments are given in parenthesis. ND, not determined.

phosphorylation, as has been reported for AtGWD3/PWD (Baunsgaard *et al.*, 2005; Kötting *et al.*, 2005).

The ratio between C-6 and C-3 phosphorylation was determined by acid hydrolysis of labelled soluble starch and separation by high-performance anion-exchange chromatography (HPAEC). Fractions collected from the peaks corresponding to glucose-6-phosphate and glucose-3-phosphate were labelled at a ratio of 86:14. It has recently been determined that phosphorylation of the C-6 and C-3 position is selectively catalysed by the GWD1 and GWD3/PWD isoforms, respectively (Ritte *et al.*, 2006). The obtained ratio shows that AtGWD2 primarily phosphorylates the C-6 position. Since maltose-6-phosphate, which is formed as a result of incomplete hydrolysis, has been shown to co-elute with glucose-3-phosphate under the conditions used, it is likely that AtGWD2 exclusively phosphorylates the C-6 position as has been observed for both AtGWD1 and potato GWD (Ritte *et al.*, 2006).

Characterization of AtGWD2 *mutants*

Three T-DNA insertion mutants in the *AtGWD2* gene were isolated from two different ecotype backgrounds. An insertion in the ecotype Wassilewskija was obtained by screening a T-DNA transformed *Arabidopsis* population from the University of Wisconsin *Arabidopsis* knockout facility (Krysan *et al.*, 1999). The insertion was mapped to exon 9 and the mutant line called *gwd2-1*. Two mutants in the Columbia (Col-0) background were identified from flanking sequence tags (FSTs). A mutant with the insert mapped to exon 15 was obtained from the GABI-Kat collection (Rosso *et al.*, 2003) and a mutant with an insertion in exon 23 was obtained from the SALK collection (Alonso *et al.*, 2003). These lines were named *Atgwd2-2* and *Atgwd2-3*, respectively. Homozygous lines were selected by PCR screening of genomic DNA and insertions were verified by PCR using primers matching the borders of the T-DNA insert and the *AtGWD2* gene. Reverse transcription (RT)-PCR analysis confirmed that none of the mutants produced a functional *AtGWD2* transcript. Plants were grown for at least three generations with no visible phenotype from an observation of growth and development when compared with the wild type. Iodine staining of leaves after the dark period did not reveal any accumulation of starch in the mutants. Enzymatic determination of starch and sugar content (glucose, fructose, and sucrose) in leaves after both the light and dark periods did not reveal any differences when compared with the wild type. In contrast to the results obtained with null mutants of *AtGWD1* and *AtGWD3/PWD* (Yu *et al.*, 2001; Baunsgaard *et al.*, 2005; Kötting *et al.*, 2005), null mutants of *AtGWD2* do not appear to be affected in degradation of transient starch under standard growth conditions.

AtGWD2 *is expressed in the companion cells of the phloem in an age-dependent manner*

Studies on the frequency and distribution of ESTs in tissues of *Arabidopsis* suggested that *AtGWD2* is expressed late in the plant life cycle. Two ESTs were isolated from a leaf senescence library (GenBank accession nos CD529796 and CD529114) and a further two were isolated from flower or silique libraries (GenBank accession nos AV564246 and AU227674). In order to investigate the precise expression pattern of *AtGWD2*, a 1207 bp promoter fragment, corresponding to the entire genomic region from the end of the upstream ORF (At4g24440) to the start codon of *AtGWD2*, was cloned in front of an enhanced green fluorescent protein-β-glucoronidase fusion (GFP-GUS). This promoter region included the 5' untranslated region, containing exon 1 and part of exon 2. The promoter construct was transformed into *Arabidopsis* wild type and the T_3 and T_4 generations were analysed by X-Gluc staining for GUS activity. A highly restricted pattern of expression was observed with strong expression in the vascular tissues of leaves, stem, roots, flowers, and siliques (Fig. 3). This vascular expression pattern was highly age-dependent in all tissues, appearing just before the onset of senescence. The first signs of GUS activity in developing *Arabidopsis* plants were seen in the cotyledons of approximately 3-week-old plants (grown in 8 h light) immediately prior to the first visible signs of senescence (i.e. yellowing). The appearance of GUS activity during development of the rosette followed this pattern, with activity appearing in the lower leaf-pairs before visible senescence symptoms were observed (Fig. 3B). At the time of emergence of the inflorescence, GUS activity could be detected in the majority of mature leaves. This age-related pattern was repeated in developing flowers and siliques (Fig. 3C–F). Activity in flowers was observed in the sepals and stamens after flower opening (Fig. 3D) and strong activity was detected in the floral organ abscission zone (Fig. 3F).

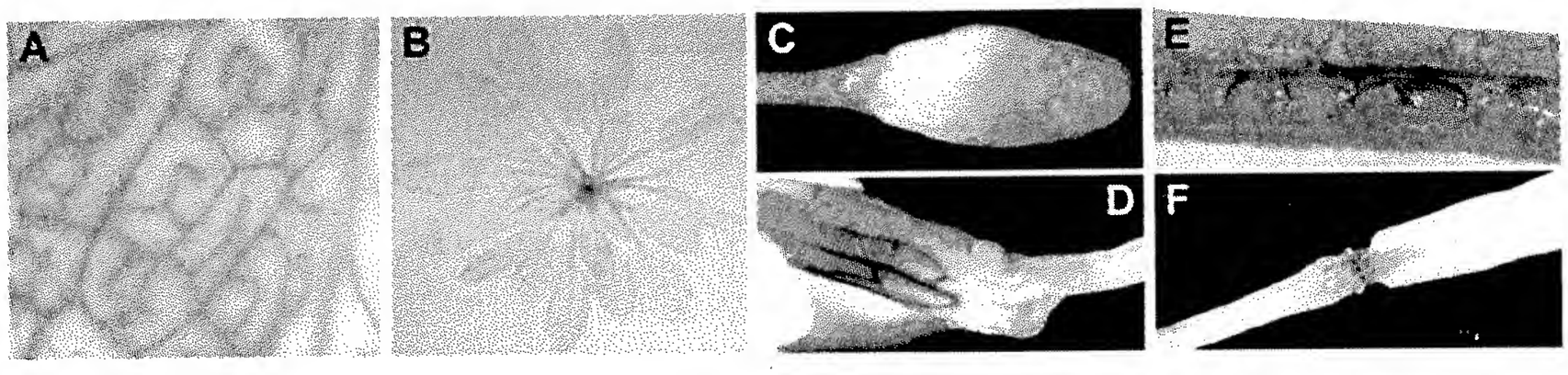

Fig. 3. GUS staining of *Arabidopsis* plants expressing a GFP-GUS fusion from the *AtGWD2* promoter. (A) A mature rosette leaf showing the vascular expression pattern. (B) A 7-week-old *Arabidopsis* plant showing expression in the lower leaf pairs. (C) Immature flower bud. (D) Mature flower with emerging silique. GUS activity can be observed in the sepals. (E) Maturing silique showing activity in the dehiscence zone between the silique walls. (F) Activity in the floral organ abscission zone after senescence of the flower and formation of the silique.

The emerging siliques retained the staining in the abscission zone during development. During silique maturation, activity appeared in the dehiscence zone between the silique walls (Fig. 3E) and in the vascular tissues of the silique walls. Cross-sections of mature leaves localized the GUS signal to the abaxial (lower) side of the primary vascular bundle, coincident with the location of the phloem (data not shown). The tissue specificity and developmental pattern of *AtGWD2* promoter activity were compared to the microarray data collected in Genevestigator (www.genevestigator.ethz.ch; Zimmermann *et al.*, 2004). The analysis revealed high levels of *AtGWD2* expression in senescent leaves, cauline leaves, siliques, and mature flower parts, in good agreement with the observed GUS activity pattern.

The GFP-GUS fusion expressed from the *AtGWD2* promoter was used to locate the specific cell types in which the *AtGWD2* promoter was active. Mature leaves of bolting plants were investigated by confocal laser scanning microscopy (CLSM). GFP fluorescence was observed in long narrow cells in the vascular bundles (Fig. 4A). These cells contained both vacuoles and chloroplasts (Fig. 4B). The presence of chloroplasts indicated that these cells were either phloem parenchyma cells or companion cells. To verify their identity, phloem sieve-plates were stained with aniline blue and their location was investigated by CLSM. Sieve-plates were observed adjacent to the GFP-labelled cells in optical cross-sections and were close to the junction between two labelled cells (Fig. 4B, inset). This confirmed the identity of the GFP-labelled cells as phloem companion cells.

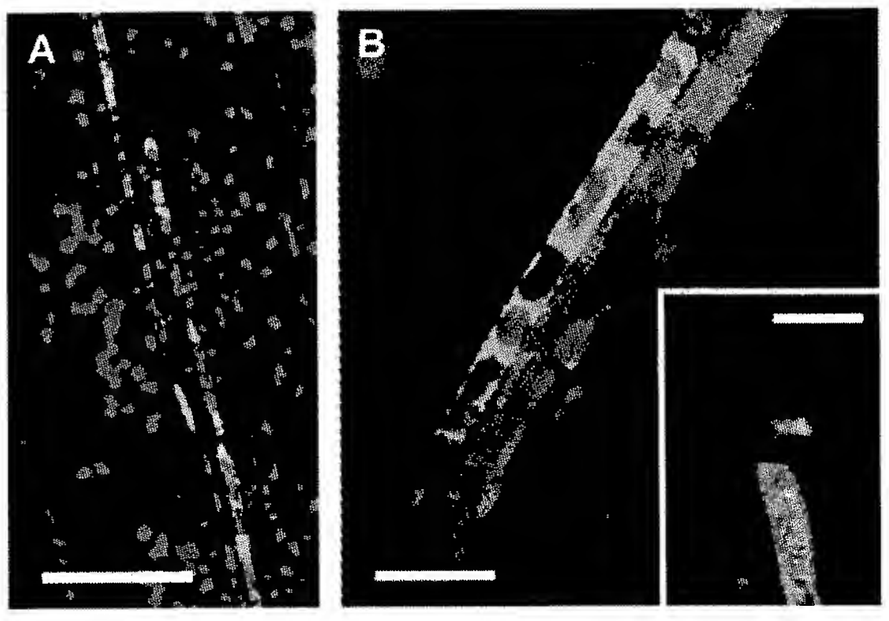

Fig. 4. Localization of the GFP-GUS fusion expressed from the *AtGWD2* promoter. (A) GFP fluorescence (green) in long narrow cells of a vascular bundle. Scale bar 40 μm. (B) Closer view of the fluorescent cells, showing chloroplasts (red) and putative vacuoles (dark 'holes'). (B, inset) Aniline blue staining of a sieve-plate (light blue) in an adjacent sieve element. Scale bar 10 μm.

AtGWD2 is not targeted to the chloroplast

As mentioned above, analysis of putative transit peptide sequences in AtGWD2 indicated that the enzyme is an extra-plastidial isoform of GWD. To determine the subcellular localization of AtGWD2, two fusions to GFP were constructed. The first construct contained the full-length AtGWD2 protein, while the second construct included the 158 N-terminal amino acids. Expression of the fusion proteins was driven by the 35S promoter. The full-length fusion was analysed by transient expression in onion epidermis and stable transformation of *Arabidopsis*. None of these approaches gave any visible GFP signal by either conventional fluorescence microscopy or CLSM. However, the AtGWD2 (aa1–158)-GFP fusion protein gave rise to clear fluorescence in several transgenic *Arabidopsis* lines when viewed with CLSM. The fluorescence was primarily restricted to the epidermal cell layer and the GFP signal was present in the nucleus and in a narrow band along the cell wall (Fig. 5A). This pattern coincides with that of free GFP (Haseloff *et al.*, 1997) and suggests a cytoplasmic localization of the fusion protein. Analysis of guard cells showed clear GFP activity outside the chloroplasts (Fig. 5B), supporting the results of the transit peptide predictions.

As a second approach, full-length AtGWD2 and a series of three C-terminally truncated versions (carrying N-terminal fragments including 610, 158, and 61 amino acids, respectively) were fused to YFP and examined using a tobacco transient expression system. The two fusions containing the full-length AtGWD2 and 610 N-terminal amino acids did not give rise to any visible

fluorescence, similar to what was observed for the full-length fusion in *Arabidopsis*. The 158 and 61 amino acids fusions showed identical localization patterns with clear fluorescence in both epidermal and mesophyll cells. In epidermal cells the YFP signal was similar to the GFP signal observed in *Arabidopsis*, with fluorescence along the cell wall and in the nucleus (data not shown). In mesophyll cells the signal was clearly located outside the chloroplasts (Fig. 5D). N-terminal addition of the 78 amino acids predicted transit peptide from AtGWD1 targeted both fusions to the chloroplasts in tobacco cells. The chloroplast targeted fusion protein carrying the 158 N-terminal amino acids of AtGWD2 was located at the surface of rounded structures, presumed to be starch granules, inside the chloroplasts (Fig. 5C). This fusion protein contains one of the N-terminal starch binding domains of AtGWD2 and the binding indicates that this domain is functional *in vivo*. To verify that the cytoplasmic localization was not simply due to the loss of N-terminal targeting information caused by proteolytic breakdown of the fusion protein, western blotting was performed using a GFP-antibody. Both fusions gave a strong band of the correct size, with only a minor breakdown product in the AtGWD2 (aa1–158)-GFP fusion (Fig. 5E).

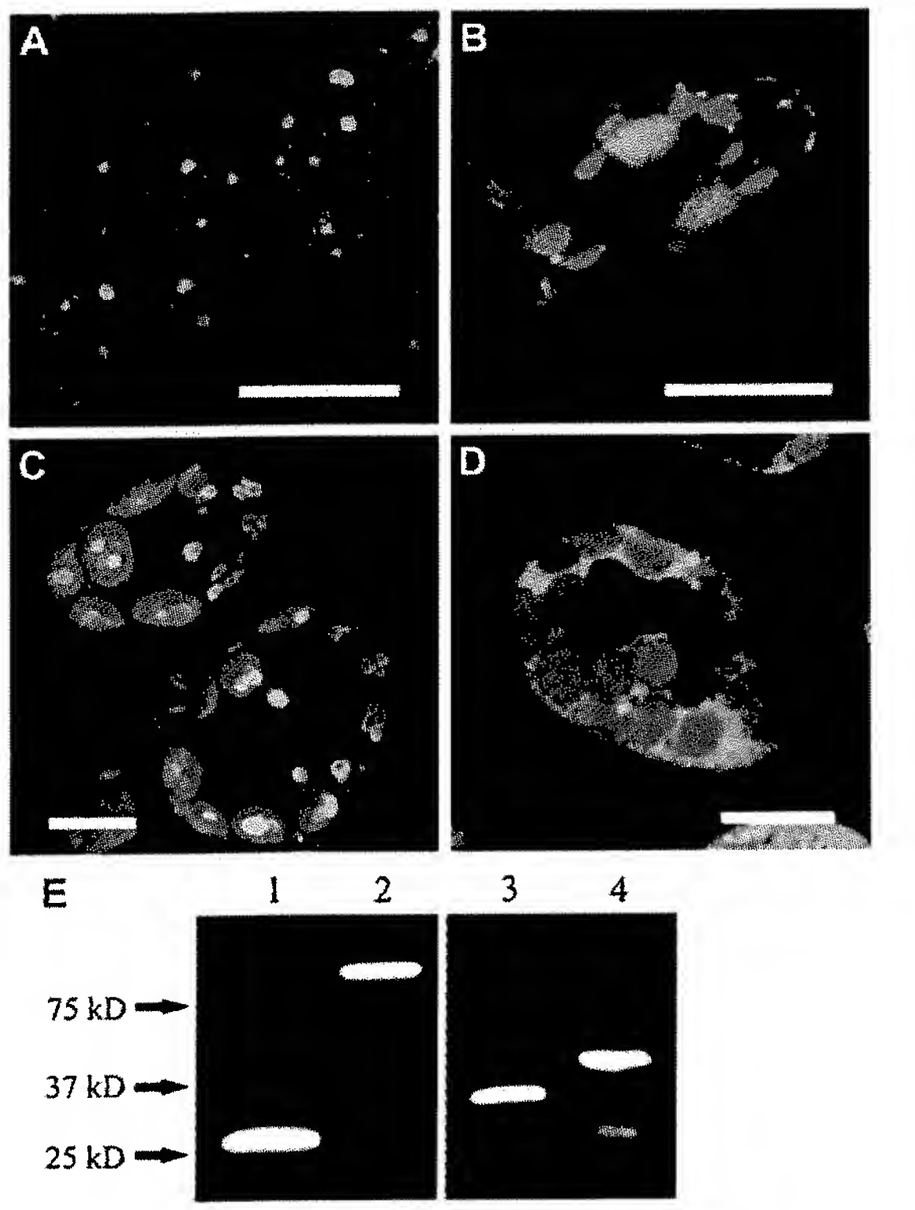

Fig. 5. Localization of fusion proteins between AtGWD2 and GFP/YFP. (A) *Arabidopsis* expressing the AtGWD2 (aa1–158)-GFP fusion in epidermal cells. GFP fluorescence (green) can be observed along the cell walls and in the nuclei. (B) An *Arabidopsis* guard cell pair. The fusion protein does not co-localize with the chloroplasts (red). (C, D) Tobacco mesophyll cells transiently expressing the AtGWD2 (aa1–158)-YFP fusion with (C) or without (D) the AtGWD1 transit peptide. Scale bars: (A) 50 μm; (B, C, D) 10 μm. (E) Western blot of the fusion proteins expressed in tobacco using a GFP antibody. Expression controls with free GFP (1) and a GFP-GUS fusion (2) driven by the 35S promoter. C-terminal YFP fusion proteins containing 61 amino acids (3) or 158 amino acids (4) of the AtGWD2 N-terminal end.

To corroborate the results of the AtGWD2-GFP/YFP fusion experiments, chloroplast import studies were performed to examine the localization of AtGWD2. Full-length AtGWD2 was transcribed and translated in the presence of radiolabelled [^{3}H]leucine *in vitro* and incubated with intact chloroplasts (C) isolated from pea seedlings. After incubation, the chloroplasts were treated with thermolysine (C+) which degrades the non-imported precursor proteins leaving the chloroplast structure intact. Chloroplasts were then fractionated into a stromal fraction (S) and a thylakoid membrane fraction (T). Fractions were loaded onto a SDS-PAGE gel and subjected to autoradiography. The resulting autoradiogram showed that the AtGWD2 protein (Fig. 6; GWD2 panel, lane C) was completely degraded by thermolysine treatment after incubation with intact chloroplasts (Fig. 6; GWD2 panel, lane C+) suggesting that AtGWD2 does not contain an *in vitro* functional transit peptide allowing import into the chloroplast. In contrast to these results, a control construct with the AtGWD1 transit peptide fused to the N-terminus of AtGWD2 was *in vitro* imported and gave a labelled double band around the correct size (~150 kDa) in the intact chloroplast preparations (Fig. 6; TP-GWD2 panel, lanes C and C+) and in the stroma (Fig. 6; TP-GWD2 panel, lane S). The double band may be due to a plastidic proteolytic activity acting on the imported translation product or alternatively, a post-translational modification of the protein. Compared with the unmodified AtGWD2, the fusion products were protected from thermolysine

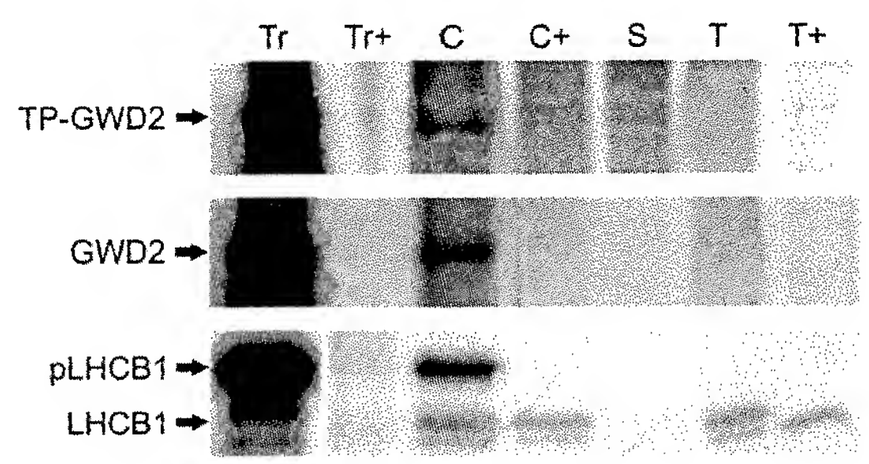

Fig. 6. Chloroplast import assays on native AtGWD2 and AtGWD2 fused to the transit peptide of AtGWD1 (TP-GWD2). Constructs were transcribed and translated *in vitro* in the presence of [^{3}H]leucine and subsequently incubated with isolated intact pea chloroplasts. The LHCB1 protein (light-harvesting chlorophyll *b* binding protein, thylakoid membrane protein) was used as an import control. The lanes correspond to *in vitro*-translated precursor (Tr), thermolysine-treated precursor (Tr+), total, washed chloroplasts immediately after import (C), thermolysine-treated chloroplasts (C+), stromal extract (S), isolated thylakoids (T), trypsin-treated thylakoids (T+).

digestion after incubation with intact chloroplasts (Fig. 6; TP-GWD2 panel, lane C+) indicating that TP-AtGWD2 was translocated into the chloroplast. The nuclear-encoded LHCB1 protein (light-harvesting chlorophyll *b* binding protein), which is targeted to the thylakoid membranes, was used as a control of the chloroplast import assay (Fig. 6; LHCB1 panel, lanes T and T+).

Sieve element starch in Arabidopsis

The specific expression of *AtGWD2* in the companion cells of the phloem prompted an investigation of the presence of starch in sieve element plastids of *Arabidopsis*. Plastids are a universal feature of sieve elements and are characterized by various types of inclusions, including starch granules (van Bel *et al.*, 2002). The function of the sieve element plastids in phloem translocation is not known, but it has been suggested that they might serve as storage units, provided that the enzymes needed for biosynthesis and degradation of the included macromolecules are present (van Bel *et al.*, 2002). Sieve element starch has previously been observed in the root protophloem of *Arabidopsis* (Wu and Zheng, 2003).

Electron microscopy (EM) was used to investigate the appearance of sieve element starch granules in *Arabidopsis* wild-type Columbia-0 and the mutant *Atgwd2-2*. Sections of the inflorescence stem showed sieve element plastids containing round starch granules with a diameter of approximately 200–300 nm (Fig. 7). Most plastids were surrounded by a seemingly intact double membrane. No differences were observed between wild type and mutant, with respect to size and morphology of starch granules (data not shown). However, the EM micrographs were not generally suitable for total quantification of sieve element starch.

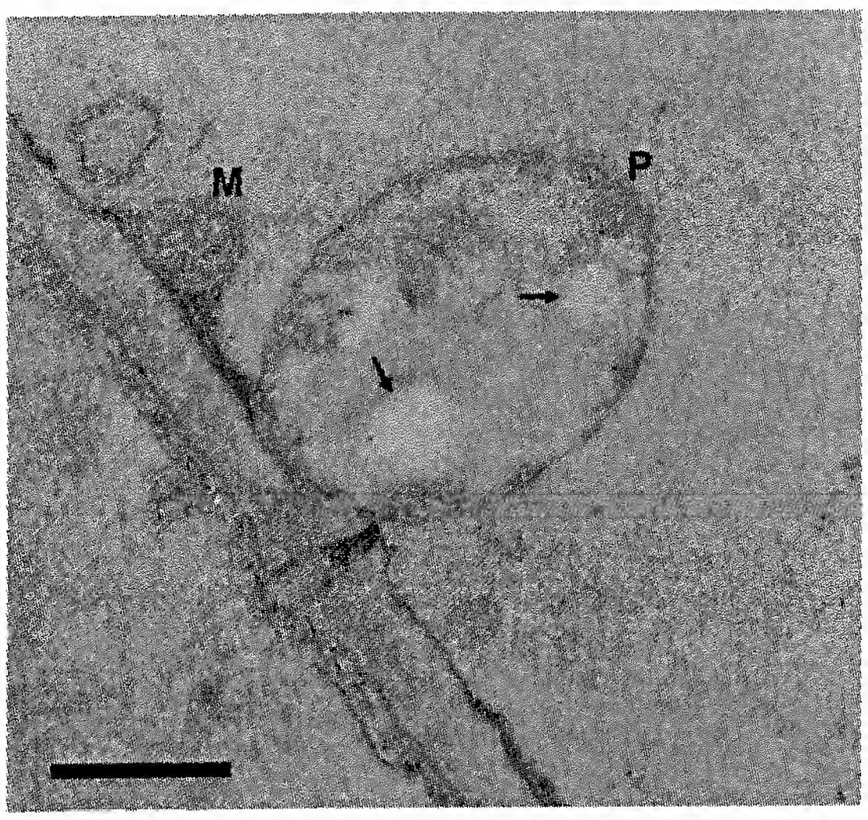

Fig. 7. Electron microscopy image of a sieve element plastid from the inflorescence of *Arabidopsis*. M, mitochondrion. P, plastid. Arrows indicate starch granules. Scale bar 500 nm.

Discussion

A search of available sequence data from higher plants revealed homologues of *AtGWD2* in three *Brassica* species and in a collection of *Citrus* sequences. This restricted pattern of appearance is intriguing as homologues of both *AtGWD1* and *AtGWD3/PWD* can be readily identified in most higher plants (Baunsgaard *et al.*, 2005). The apparent lack of homologues of *AtGWD2* among the abundance of ESTs and genomic sequences from monocot species, suggests that *AtGWD2* evolved after the divergence of the monocots and dicots. The phylogenetic tree shows that the GWD2 sequences form a group separate from the GWD1 orthologues of both monocots and dicots. This suggests a duplication of GWD before the divergence of monocots and dicots, although this does not take into account differences in evolutionary rate caused by varying selective pressure. Another, perhaps more unlikely, explanation is that the monocots have lost the gene corresponding to *AtGWD2* during the course of evolution. The continuous release of new sequence data from many plants species is likely to shed more light on this question in the future.

In vitro analysis of purified enzyme demonstrated that AtGWD2 was active on elongated glucan chains and did not require previous phosphorylation of the substrate. This substrate preference resembles that of potato GWD (Ritte *et al.*, 2002; Mikkelsen *et al.*, 2004). Furthermore, AtGWD2 primarily phosphorylated the C-6 position of the glycosyl residues. These results, along with the data that indicate that AtGWD2 is an extra-plastidial enzyme, support the idea that AtGWD2 is an active cytosolic isoform of AtGWD1. Analysis of *Arabidopsis* mutants demonstrated that the enzyme is not required for the degradation of transient starch, suggesting that AtGWD2 is active on an, as yet unidentified, glucan substrate.

AtGWD2 promoter activity was restricted to the companion cells of the phloem and was highly age-dependent. The expression followed the development of senescence in leaves, flowers, and siliques and was usually observed just before the appearance of visible senescence symptoms. The link with senescence suggests that the AtGWD2 enzyme might be involved in the breakdown of starch or starch-like structures during the withdrawal of nutrients from the senescing leaf. The specific expression in companion cells could implicate AtGWD2 in either the transport of carbohydrates through the phloem or in the degradation of phloem-specific structures. Presently, there is no specific evidence for the existence of large α-linked polysaccharides, other than starch, in phloem tissues. It is possible that the cytosolic soluble heteroglycan that has

been identified in *Arabidopsis* (Fettke *et al.*, 2005) is also present in companion cells and phloem parenchyma cells, but there is no evidence to suggest that α-glucan, water dikinase activity would be required for its metabolism.

The observation that the major form of β-amylase in *Arabidopsis* is localized in the phloem sieve elements lead to the idea that β-amylase activity might play a role in preventing build-up of polymerized polysaccharides that would impede flow through the sieve-plates (Wang *et al.*, 1995). Given the location of AtGWD2 and the RAM1 β-amylase in *Arabidopsis* it is tempting to speculate that they might function in the metabolism of larger polysaccharides in the phloem sieve elements, either as a way of preventing their build-up or as a way of regulating the transport and availability of sugars. Proteins present in sieve elements are synthesized in companion cells and transferred via plasmodesmata. The size of the AtGWD2 protein would most likely prevent non-specific (passive) trafficking between these two cell types (Lough and Lucas, 2006), but experiments with *Cucurbita maxima* have shown that phloem exudate contains proteins ranging in molecular weight from 10–200 kDa (Balachandran *et al.*, 1997). How this specific (selective) trafficking of proteins destined for the sieve element is accomplished is unknown. Many phloem proteins can modify the size exclusion limit of mesophyll plasmodesmata enabling transport of larger proteins and compounds (Balachandran *et al.*, 1997). There is also good evidence to suggest that selective trafficking can be mediated by chaperones or shuttle-proteins that target the selected proteins to the plasmodesmal channel (Lee *et al.*, 2003). Furthermore, transport of the encoding mRNA to the sieve element has been described for a number of proteins, among them the sucrose transporter SUT1 from potato (Lough and Lucas, 2006). The SUT1 protein is present in sieve elements, but transcription occurs in companion cells and the mRNA is found in both cell types (Kühn *et al.*, 1997). Whether the transported mRNA gives rise to any protein in the sieve element is still unresolved. Although these data show that the *AtGWD2* promoter is active in companion cells, a sensitive anti-AtGWD2 antibody would be required to analyse whether or not the protein itself resides in sieve elements where RAM1 has been localized (Wang *et al.*, 1995). The lack of any clear phenotype in null mutants of *AtGWD2* and *RAM1* (Laby *et al.*, 2001) suggests that their contribution to sugar metabolism under normal circumstances is minor. The expression of *RAM1* is heavily up-regulated in response to sucrose, indicating that sucrose affects the amount of RAM1 substrate (Mita *et al.*, 1995). Induction of *AtGWD2* promoter activity has been observed in seedlings germinated on sucrose-containing media, suggesting a similar response of *AtGWD2* (data not shown).

Both GWD and isoamylase sequences have been proposed to be a prerequisite for the appearance of semi-crystalline starch-like polymers (Coppin *et al.*, 2005), since these enzymes distinguish plant starch metabolism from the glycogen metabolism of animals, fungi, and bacteria. The presence of *GWD*s appears to be a ubiquitous feature of all organisms accumulating semi-crystalline storage polysaccharides. Homologues of *GWD* can be found in plants, the green and red algae, and in apicomplexan parasites (Mikkelsen *et al.*, 2004; Ral *et al.*, 2004; Coppin *et al.*, 2005). If the existence of GWDs is a prerequisite for the successful metabolism of semi-crystalline polysaccharides, it is tempting to assume that AtGWD2 acts on such a substrate *in vivo*. The starch granules in the plastids of *Arabidopsis* phloem sieve elements present an appealing target for the action of AtGWD2. It has been determined that sieve element starch in bean hypocotyls contains a high proportion of α-1,6 linkages and is structurally distinct from ordinary starch (Palevitz and Newcomb, 1970). The sieve element plastid membrane degrades during development of root protophloem in *Arabidopsis* leaving starch granules free in the lumen (Wu and Zheng, 2003). Older sieve elements in bean also contain starch granules free in the lumen, but the authors could not conclude whether they were released naturally during ageing or the result of cutting and fixing the tissue (Palevitz and Newcomb, 1970). Pressure release in fava bean sieve elements leads to immediate rupture of the plastids. It was speculated that the liberated contents of the sieve element plastids, including the starch granules, might aid in plugging the sieve pore in response to wounding (Knoblauch and van Bel, 1998). The apparent lack of a chloroplast transit peptide and the late expression in the plant life cycle could suggest that AtGWD2 acts on starch granules released from degrading plastids in ageing plants. The structure of sieve element plastids in the inflorescence stem of *Arabidopsis* was investigated. Although the plastids were still surrounded by an apparently intact double membrane, the nature and integrity of this membrane is unknown. Starch granules were present in both wild type and an *Atgwd2* mutant, but because the plane of sectioning in EM does not necessarily pass through the centre of the granule, quantification of the results can be difficult. Detecting any differences in the number or size distribution of sieve element starch granules in wild type and mutant would require a more comprehensive quantitative survey. It is worth noting that many plant species, particularly among the monocots, do not contain starch in the sieve element plastids (Behnke, 2003).

Acknowledgements

We thank Lis B Møller, Per Lassen Nielsen, and Lise Girsel for technical assistance and René Mikkelsen for valuable advice and discussions. RIKEN Genomic Sciences Center is gratefully acknowledged for providing the AtGWD2 full-length cDNA clone. This

project was supported by a grant from The Danish Research Council for Technology and Production Sciences (Grant no. 23-04-0239).

References

Alonso JM, Stepanova AN, Leisse TJ, *et al.* 2003. Genome-wide insertional mutagenesis of *Arabidopsis thaliana*. *Science* **301,** 653–657.

Balachandran S, Xiang Y, Schobert C, Thompsom GA, Lucas WJ. 1997. Phloem sap proteins from *Cucurbita maxima* and *Ricinus communis* have the capacity to traffic cell to cell through plasmodesmata. *Proceedings of the National Academy of Sciences, USA* **94,** 14150–14155.

Baunsgaard L, Lütken H, Mikkelsen R, Glaring MA, Pham TT, Blennow A. 2005. A novel isoform of glucan, water dikinase phosphorylates pre-phosphorylated α-glucans and is involved in starch degradation in *Arabidopsis*. *The Plant Journal* **41,** 595–605.

Behnke HD. 2003. Sieve-element plastids and evolution of monocotyledons, with emphasis on Melanthiaceae sensu lato and Aristolochiaceae-Asaroideae, a putative dicotyledon sister group. *Botanical Reviews* **68,** 524–544.

Blennow A, Bay-Smidt AM, Olsen CE, Møller BL. 1998. Analysis of starch bound glucose 3-phosphate and glucose 6-phosphate using controlled acid treatment combined with high-performance anion-exchange chromatography. *Journal of Chromatography A* **829,** 385–391.

Blennow A, Nielsen TH, Baunsgaard L, Mikkelsen R, Engelsen SB. 2002. Starch phosphorylation: a new front line in starch research. *Trends in Plant Science* **7,** 445–450.

Chia T, Thorneycroft D, Chapple A, Messerli G, Chen J, Zeeman SC, Smith SM, Smith AM. 2004. A cytosolic glucosyltransferase is required for conversion of starch to sucrose in *Arabidopsis* leaves at night. *The Plant Journal* **37,** 853–863.

Coppin A, Varré JS, Lienard L, Dauvillée D, Guérardel Y, Soyer-Gobillard MO, Buléon A, Ball S, Tomavo S. 2005. Evolution of plant-like crystalline storage polysaccharides in the protozoan parasite *Toxoplasma gondii* argues for a red alga ancestry. *Journal of Molecular Evolution* **60,** 257–267.

Delatte T, Umhang M, Trevisan M, Eicke S, Thorneycroft D, Smith SM, Zeeman SC. 2006. Evidence for distinct mechanisms of starch granule breakdown in plants. *Journal of Biological Chemistry* **281,** 12050–12059.

Edner C, Li J, Albrecht T, *et al.* 2007. Glucan, water dikinase activity stimulates breakdown of starch granules by plastidial β-amylases. *Plant Physiology* **145,** 17–28.

Emanuelsson O, Nielsen H, Brunak S, von Heijne G. 2000. Predicting subcellular localization of proteins based on their N-terminal amino acid sequence. *Journal of Molecular Biology* **300,** 1005–1016.

Fettke J, Chia T, Eckermann N, Smith A, Steup M. 2006. A transglucosidase necessary for starch degradation and maltose metabolism in leaves at night acts on cytosolic heteroglycans (SHG). *The Plant Journal* **46,** 668–684.

Fettke J, Eckermann N, Tiessen A, Geigenberger P, Steup M. 2005. Identification, subcellular localization and biochemical characterization of water-soluble heteroglycans (SHG) in leaves of *Arabidopsis thaliana* L.: distinct SHG reside in the cytosol and in the apoplast. *The Plant Journal* **43,** 568–585.

Haseloff J, Siemering KR, Prasher DC, Hodge S. 1997. Removal of a cryptic intron and subcellular localization of green fluorescent protein are required to mark transgenic *Arabidopsis* plants brightly. *Proceedings of the National Academy of Sciences, USA* **94,** 2122–2127.

Kaplan F, Guy CL. 2005. RNA interference of *Arabidopsis* beta-amylase8 prevents maltose accumulation upon cold shock and increases sensitivity of PSII photochemical efficiency to freezing stress. *The Plant Journal* **44,** 730–743.

Karimi M, Inzé D, Depicker A. 2002. GATEWAY™ vectors for *Agrobacterium*-mediated plant transformation. *Trends in Plant Science* **7,** 193–195.

Knoblauch M, van Bel AJE. 1998. Sieve tubes in action. *The Plant Cell* **10,** 35–50.

Kötting O, Pusch K, Tiessen A, Geigenberger P, Steup M, Ritte G. 2005. Identification of a novel enzyme required for starch metabolism in *Arabidopsis* leaves. The phosphoglucan, water dikinase. *Plant Physiology* **137,** 242–252.

Kühn C, Franceschi VR, Schulz A, Lemoine R, Frommer WB. 1997. Macromolecular trafficking indicated by localization and turnover of sucrose transporters in enucleate sieve elements. *Science* **275,** 1298–1300.

Kumar S, Tamura K, Nei M. 2004. MEGA3: Integrated software for molecular evolutionary genetics analysis and sequence alignment. *Briefings in Bioinformatics* **5,** 150–163.

Krysan PJ, Young JK, Sussman MR. 1999. T-DNA as an insertional mutagen in *Arabidopsis*. *The Plant Cell* **11,** 2283–2290.

Laby RJ, Kim D, Gibson SI. 2001. The *ram1* mutant of *Arabidopsis* exhibits severely decreased β-amylase activity. *Plant Physiology* **127,** 1798–1807.

Lee JY, Yoo BC, Rojas MR, Gomez-Ospina N, Staehelin LA, Lucas WJ. 2003. Selective trafficking of non-cell-autonomous proteins mediated by NtNCAPP1. *Science* **299,** 392–396.

Lloyd JR, Kossman J, Ritte G. 2005. Leaf starch degradation comes out of the shadows. *Trends in Plant Science* **10,** 130–137.

Lorberth R, Ritte G, Willmitzer L, Kossman J. 1998. Inhibition of a starch-granule-bound protein leads to modified starch and repression of cold sweetening. *Nature Biotechnology* **16,** 473–477.

Lough TJ, Lucas WJ. 2006. Integrative plant biology: role of phloem long-distance macromolecular trafficking. *Annual Review of Plant Biology* **57,** 203–232.

Lu Y, Sharkey TD. 2004. The role of amylomaltase in maltose metabolism in the cytosol of photosynthetic cells. *Planta* **218,** 466–473.

Mikkelsen R, Baunsgaard L, Blennow A. 2004. Functional characterization of α-glucan, water dikinase, the starch phosphorylating enzyme. *Biochemical Journal* **377,** 525–532.

Mikkelsen R, Suszkiewicz K, Blennow A. 2006. A novel type carbohydrate-binding module identified in α-glucan, water dikinase is specific for regulated plastidial starch metabolism. *Biochemistry* **45,** 4674–4682.

Mita S, Suzuki-Fujii K, Nakamura K. 1995. Sugar-inducible expression of a gene for β-amylase in *Arabidopsis thaliana*. *Plant Physiology* **107,** 895–904.

Nielsen TH, Wischmann B, Enevoldsen K, Møller BL. 1994. Starch phosphorylation in potato tubers proceeds concurrently with *de novo* biosynthesis of starch. *Plant Physiology* **105,** 111–117.

Niittylä T, Messerli G, Trevisan M, Chen J, Smith AM, Zeeman SC. 2004. A previously unknown maltose transporter essential for starch degradation in leaves. *Science* **303,** 87–89.

Nour-Eldin HH, Hansen BG, Nørholm MHH, Jensen JK, Halkier BA. 2006. Advancing uracil-excision based cloning towards an ideal technique for cloning PCR fragments. *Nucleic Acids Research* **34,** e122.

Palevitz BA, Newcomb EH. 1970. A study of sieve element starch using sequential enzymatic digestion and electron microscopy. *Journal of Cell Biology* **45,** 383–398.

Ral JP, Derelle E, Ferraz C, *et al.* 2004. Starch division and partitioning. A mechanism for granule propagation and maintenance

in the picophytoplanktonic green alga *Ostreococcus tauri*. *Plant Physiology* **136,** 1–8.

Ritte G, Heydenreich M, Mahlow S, Haebel S, Kötting O, Steup M. 2006. Phosphorylation of C6- and C3-positions of glycosyl residues in starch is catalysed by distinct dikinases. *FEBS Letters* **580,** 4872–4876.

Ritte G, Lloyd JR, Eckermann N, Rottmann A, Kossman J, Steup M. 2002. The starch-related R1 protein is an α-glucan, water dikinase. *Proceedings of the National Academy of Sciences, USA* **99,** 7166–7171.

Ritte G, Scharf A, Eckermann N, Haebel S, Steup M. 2004. Phosphorylation of transitory starch is increased during degradation. *Plant Physiology* **135,** 1–10.

Ritte G, Steup M, Kossman J, Lloyd JR. 2003. Determination of the starch-phosphorylating enzyme activity in plant extracts. *Planta* **216,** 798–801.

Robinson C, Mant A. 2002. Import of proteins into isolated chloroplasts and thylakoid membranes. In: Gilmartin PM, Bowler C, eds. *Molecular plant biology: a practical approach*, Vol. 2. Oxford, UK: Oxford University Press, 123–146.

Rosso MG, Li Y, Strizhov N, Reiss B, Dekker K, Weisshaar B. 2003. An *Arabidopsis thaliana* T-DNA mutagenized population (GABI-Kat) for flanking sequence tag-based reverse genetics. *Plant Molecular Biology* **53,** 247–259.

Small I, Peeters N, Legeai F, Lurin C. 2004. Predotar: a tool for rapidly screening proteomes for N-terminal targeting sequences. *Proteomics* **4,** 1581–1590.

Scheidig A, Fröhlich A, Schulze S, Lloyd JR, Kossman J. 2002. Downregulation of a chloroplast-targeted β-amylase leads to a starch-excess phenotype in leaves. *The Plant Journal* **30,** 581–591.

Schulz A, Kühn C, Riesmeier JW, Frommer WB. 1998. Ultrastructural effects in potato leaves due to antisense-inhibition of the sucrose transporter indicate an apoplasmic mode of phloem loading. *Planta* **206,** 533–543.

Smith AM, Zeeman SC, Smith SM. 2005. Starch degradation. *Annual Review of Plant Biology* **56,** 73–98.

van Bel AJE, Ehlers K, Knoblauch M. 2002. Sieve elements caught in the act. *Trends in Plant Science* **7,** 126–132.

Voinnet O, Rivas S, Mestre P, Baulcombe D. 2003. An enhanced transient expression system in plants based on suppression of gene silencing by the p19 protein of tomato bushy stunt virus. *The Plant Journal* **33,** 949–956.

Wang Q, Monroe J, Sjölund RD. 1995. Identification and characterization of a phloem-specific β-amylase. *Plant Physiology* **109,** 743–750.

Weise SE, Weber APM, Sharkey TD. 2004. Maltose is the major form of carbon exported from the chloroplast at night. *Planta* **218,** 474–482.

Wu H, Zheng XF. 2003. Ultrastructural studies on the sieve elements in root protophloem of *Arabidopsis thaliana*. *Acta Botanica Sinica* **45,** 322–330.

Yu TS, Kofler H, Häusler RE, *et al.* 2001. The *Arabidopsis sex1* mutant is defective in the R1 protein, a general regulator of starch degradation in plants, and not in the chloroplast hexose transporter. *The Plant Cell* **13,** 1907–1918.

Yu TS, Zeeman SC, Thorneycroft D, *et al.* 2005. α-amylase is not required for breakdown of transitory starch in *Arabidopsis* leaves. *Journal of Biological Chemistry* **280,** 9773–9779.

Zeeman SC, Smith SM, Smith AM. 2007. The diurnal metabolism of leaf starch. *Biochemical Journal* **401,** 13–28.

Zeeman SC, Thorneycroft D, Schupp N, Chapple A, Weck M, Dunstan H, Haldimann P, Bechtold N, Smith AM, Smith SM. 2004. Plastidial α-glucan phosphorylase is not required for starch degradation in *Arabidopsis* leaves but has a role in the tolerance of abiotic stress. *Plant Physiology* **135,** 1–10.

Zimmermann P, Hirsch-Hoffmann M, Hennig L, Gruissem W. 2004. GENEVESTIGATOR. *Arabidopsis* microarray database and analysis toolbox. *Plant Physiology* **136,** 2621–2632.